

Cell Shape and Forces in Elastic and Structured Environments: From Single Cells to Organoids

Rabea Link, Kai Weißenbruch, Motomu Tanaka, Martin Bastmeyer,*
and Ulrich S. Schwarz*

With the advent of mechanobiology, cell shape and forces have emerged as essential elements of cell behavior and fate, in addition to biochemical factors such as growth factors. Cell shape and forces are intrinsically linked to the physical properties of the environment. Extracellular stiffness guides migration of single cells and collectives as well as differentiation and developmental processes. In confined environments, cell division patterns are altered, cell death or extrusion might be initiated, and other modes of cell migration become possible. Tools from materials science such as adhesive micropatterning of soft elastic substrates or direct laser writing of 3D scaffolds have been established to control and quantify cell shape and forces in structured environments. Herein, a review is given on recent experimental and modeling advances in this field, which currently moves from single cells to cell collectives and tissue. A very exciting avenue is the combination of organoids with structured environments, because this will allow one to achieve organotypic function in a controlled setting well suited for long-term and high-throughput culture.

hormones, and cytokines has been appreciated from the very start of cell culture experiments, the insight that spatial control of cell adhesion, the physical properties of the extracellular matrix as well as the mechanics of the cytoskeleton and the nucleus might be equally important for cellular decision making are rather recent insights. Not surprisingly, it was tied to the development of new tools that allowed researchers to control the extracellular environment. This development started by transferring tools from the microfabrication of electronic devices into the life sciences, most notably microcontact printing to generate adhesive islands to control cell adhesion to planar substrates.^[2] Pioneering work showed that cell fate can be controlled by the size of the adhesive islands: cells only survived on large islands and triggered apoptosis on small ones.^[3] Later it was discovered that this switch is related to the translation of the transcription factor YAP/TAZ into the nucleus in mechanically stressed cells.^[4]

Apart from geometry, extracellular stiffness has been found to be a major regulator of cell behavior, and again this insight was tight to advances in materials preparation. Soft elastic substrates were introduced into cell culture mainly to measure cell forces from their deformations.^[5,6] However, it was then realized

1. Introduction

During the last decades, cell mechanics, forces, and shape have emerged as important elements of the way biological cells interact with their environment.^[1] While the importance of control of cells through biochemical ligands such as growth factors,

R. Link, U. S. Schwarz
Institute for Theoretical Physics
Heidelberg University
69120 Heidelberg, Germany
E-mail: ulrich.schwarz@bioquant.uni-heidelberg.de

R. Link, U. S. Schwarz
BioQuant-Center
Heidelberg University
69120 Heidelberg, Germany

K. Weißenbruch, M. Bastmeyer
Zoological Institute
Karlsruhe Institute of Technology (KIT)
76131 Karlsruhe, Germany
E-mail: martin.bastmeyer@kit.edu

K. Weißenbruch, M. Bastmeyer
Institute for Biological and Chemical Systems
Biological Information Processing
Karlsruhe Institute of Technology (KIT)
76344 Karlsruhe, Germany

M. Tanaka
Institute of Physical Chemistry
Heidelberg University
69120 Heidelberg, Germany

 The ORCID identification number(s) for the author(s) of this article can be found under <https://doi.org/10.1002/adfm.202302145>

© 2023 The Authors. Advanced Functional Materials published by Wiley-VCH GmbH. This is an open access article under the terms of the Creative Commons Attribution-NonCommercial-NoDerivs License, which permits use and distribution in any medium, provided the original work is properly cited, the use is non-commercial and no modifications or adaptations are made.

DOI: 10.1002/adfm.202302145

that substrate stiffness has a profound influence on single cell organization and migration^[7] as well as on differentiation.^[8,9] Like on large islands, cells on stiffer substrates spread better, and YAP/TAZ is translocated into the nucleus.^[4,10] It was also shown that extracellular stiffness affects the migration of cell collectives, which often behave as an effective supracell that can sense more shallow stiffness gradients than single cells.^[11] Together, these historical developments prove that tools from materials science can be instrumental for promoting progress in the life sciences. In particular, they open the door for novel biomedical applications and therapies like analysis of patient samples and tissue regeneration in the test tube.

Since its inception around three decades ago, the field of mechanobiology has seen dramatic growth, with many new tools and model systems entering the field. Most importantly, we have seen a shift from single cell studies to work with cell collectives, cell monolayers, 3D model tissue, and organoids.^[12–16] As the field moved from 2D to 3D, imaging and force measurements became more challenging, but were met by new technologies. To image 3D cell assemblies, light sheet and two-photon microscopies have been helpful.^[17–19] Today forces can be measured in situ by inserting oil droplets^[20] or elastic microbeads^[21] into tissue. Optogenetics can be used to control cell forces in space and time.^[22] Direct laser writing of 3D scaffolds has been adapted to cell culture conditions and used to control cell shape and forces in 3D.^[23,24] More recently, microfabrication has been used to control the organization of organotypic systems^[25] and organoids in 3D.^[26] Here we will review these recent advances. In addition, we will discuss how they can be used to develop and parametrize mathematical models, which in the future are expected to become more predictive regarding optimal design.^[27] We will start by discussing single cells in Section 2, then proceed to cell collectives and monolayers in Section 3, and finally discuss organoids and organotypic cultures in Section 4. We will conclude with a summary and outlook in Section 5.

2. Single Cells

Single cells are the fundamental building blocks of life. While there is an enormous diversity in animal species and their cell types, the cytoskeleton, which is determining its mechanics and shape, is strikingly universal. It is primarily made up of three different filament systems: actin filaments, which together with the molecular motor myosin II are responsible for contractility and motility; microtubules, which are important for positioning of organelles and directed transport processes within the cell; and intermediate filaments, which reinforce and complement the mechanics provided by actin and microtubules, especially in epithelial monolayers, which have to perform under very large strains.^[28] While each filament system is well-investigated by itself, the interplay between them is the topic of much on-going research.^[29] Very importantly, cell mechanics are also strongly determined by the mechanics of the nucleus, which is typically ten times stiffer than the cytoplasm and tightly integrated with the cytoskeleton through the LINC-complexes.^[30] It has been argued earlier that cells have to use their cytoskeleton to sense and calibrate mechanical cues from their environment,^[31] and today the nucleus should be added as an additional measurement devise.^[32,33]

With the help of rationally designed cell environments, the exact impact of physical cues, such as substrate geometry and stiffness, on cell organization, mechanics, behavior, and fate can be investigated. The best-understood subsystem is cell adhesion to the extracellular matrix.^[34] Transmembrane proteins from the integrin-family located on the cell surface enable cells to adhere to extracellular matrix proteins such as fibronectin or collagen. Through a large number of adaptor proteins, the integrins are mechanically connected to the actin cytoskeleton.^[35] Using the myosin II molecular motors, the actin cytoskeleton of the adhered cell contracts, therefore pulling on its environment to test substrate stiffness,^[36,37] adhesive areas,^[3] geometry,^[38] and curvature.^[39] The signaling pathway from local force sensing to global cell changes is not yet fully understood, but it is clear that large-scale structures such as stress fibers and the nucleus play an important role as integrative elements. Cell-level effects have been observed for different cell types and on different lengths and time scales: the mechanical microenvironment can lead to polarization via symmetry breaking,^[40] remodeling of the cytoskeleton,^[41–43] traction force distribution,^[44] and durotaxis.^[36,45]

2.1. Effect of Extracellular Stiffness on Single Cells

While traditional cell culture works with stiff glass or polystyrene substrates, during the last decades soft elastic substrates have been established to expose single cells to physiological stiffness values or even to stiffness gradients.^[46] An appropriate choice is hydrogels, which are hydrophilic polymer networks that are able to absorb large amounts of water, which gives them mechanical and chemical properties similar to the natural cell environment. Hydrogels can be manufactured to have elasticities similar to physiological tissue.^[47] Due to their high water content, nutrients and other soluble factors can be transported to and away from the cell.^[48] The large amount of water in hydrogels leads to optical clarity, which thus allows for microscopy through the hydrogel. Hydrogels are often produced from synthetic polymers because naturally derived hydrogels have high variability in their physical and chemical parameters. However, while the global properties of synthetic hydrogels can be measured and engineered with high precision, the local microenvironment of the single cell inside both naturally derived and synthetic hydrogels is not necessarily reproducible.^[49,50] Hydrogels also lead to water flow under cell traction, which makes quantitative analysis challenging in certain situations.^[51] Because cells locally exert nN-forces onto their environment through μm -sized focal adhesions, one needs elastic substrates with a Young modulus $\approx \text{nN } \mu\text{m}^{-2} = \text{kPa}$ to measure these forces.^[52] For the widely used polyacrylamide (PAA) system, different combinations of monomer and crosslinker concentrations can achieve such values.^[53,54] In order to avoid water flow through hydrogels and also to achieve more optical contrast at the substrate-medium interface, for example to perform reflection interference contrast microscopy,^[55] one can use elastic substrates made from the rubber material polydimethylsiloxane (PDMS). However, it is notoriously difficult to achieve stiffness in the sub-kPa for PDMS, because here the material becomes very sticky and viscous. Therefore, different formulations with longer polymer chains have been developed.^[56]

Early work in this field used mainly PAA and revealed that focal adhesions and stress fibers develop well only on stiffer substrates, with the crossover typically at a few kPa.^[7] It was then found that substrate stiffness also affects cell differentiation.^[8,57] Later, the nuclear translocation of YAP/TAZ has been revealed as the underlying molecular mechanism.^[4,10] When working with elastic substrates, it is important to keep in mind that different bulk elasticities typically correspond to different surface properties, such as roughness and porosity, thus potentially convoluting global and local properties. However, it has been shown experimentally that cells respond mainly to the bulk properties of the elastic substrates,^[58] validating the notion that they gain information by performing an elastic test on their environment.

2.2. Single Cells in 2D Structured Environments

While the advent of mechanobiology was strongly fostered by the insight that soft elastic substrates can have a dramatic effect on cell behavior and fate, the same holds true for geometrical and topographical cues. The effect of structured environments on single cell behavior was first studied in 2D culture for single cells using adhesive micropatterning.^[3] The main advantage of this method is that it produces precisely reproducible mechanical environments and therefore allows for experiments that lead to statistically relevant results. Adhesive micropatterns initially were produced by microcontact printing, but today are often generated with photolithography or laser-based methods.^[59] The biggest challenge of these approaches is not necessarily to functionalize the materials with adhesion molecules, but rather to find materials with anti-fouling properties that reliably passivate the non-adhesive regions. Frequently used repulsive molecules comprise BSA, Pluronic, and PLL-PEG. Moreover, gold-thiol-based chemistry can be used to fabricate patterned self-assembled monolayers with distinct hydrophilic and hydrophobic areas on gold-coated coverslips.^[60] However, the necessary gold coating restricts these methods to glass coverslips.

A zoo of interesting shapes has been established that today allows us to investigate important biological questions with high resolution, like V-shapes for cell spreading, crossbows for polarized cells, and H-patterns for cell doublets. Because cells have only a limited amount of cytoskeletal and membrane material available, the size of these patterns must be adapted to the cell type under consideration. Once these reservoirs are exhausted, the cells run into the danger of, for example, rupturing its own membranes.^[61]

A prime example of the power of 2D adhesive substrates is the study of stress fibers, which are contractile actin bundles formed by many animal cell types. As an example, **Figure 1a,a'** shows a cell on an adhesive cross pattern, where the stress fibers form as invaginations at the positions where the cell has to bridge over non-adhesive areas. This experiment reinforces the early insight that micropatterns can be used to control the exact position of stress fibers.^[43] By varying the shape of the adhesive areas, the authors showed that stress fibers grow predominantly along non-adhesive edges and that the strength of stress fibers depends on the distance between adhesive sites and the number of stress fibers in the cell. Furthermore, they were able to observe the spreading of a single cell on the micropattern, which

revealed an approximately linear increase of the curvature radius over time. In the absence of stress fibers, cell shape invagination along non-adhesive edges is increased, showing that actin stress fibers counteract the contracting cell cortex and tend to pull the boundary straight.

Stress fiber growth, organization, and force transmission is still a very active area of research, but today focuses more on the underlying mechanisms. It has been known for many years that stress fibers are formed by merging small actin bundles moving through the cytoplasm,^[62] thus the formation of the stress fiber network in single cells is a complex process and difficult to predict. Micropatterns were used to provide reproducible environments for cells to spread, which allowed the prediction of stress fiber networks of cells on micropatterns from the cell spreading history.^[63] To better understand stress fiber self-organization in stationary cells, Jalal and colleagues plated fibroblasts on circular micropatterns, see **Figure 1b,b'**. Using live cell imaging, they observed transitions between circular, radial, and linear orientations and show that they depend on molecular players such as non-muscle myosin II and α -actinin.^[64,65]

Micropatterns are often used to observe cell polarization and migration under reproducible conditions. In the “world cell race”, over 50 cell types were placed on fibronectin-coated tracks, see **Figure 1c,c'**, and their polarization, speed, and persistence were evaluated, revealing a universal correlation between speed and persistence.^[66,69] By gradually increasing the density of adhesive sites, see **Figure 1d,d'**, Autenrieth and colleagues showed that the well-known process of haptotaxis, where fibroblast cells move in the direction of the highest ECM protein concentration, holds true for discrete adhesive sites as well.^[70] Brückner and colleagues used a two-state micropattern, see **Figure 1e,e'**, to show that the motion of a single cell through a constriction has both deterministic and stochastic contributions.^[67] While wildtype cells were crossed by stochastic transitions between two stable states, cancer cells were deterministically driven over the bridges in an oscillatory manner.

To measure cell forces in micropatterning experiments, one can combine planar soft elastic substrates with adhesive micropatterning.^[71,72] From the deformations of the elastic substrate, the cellular forces are calculated using the deformation of the micropatterns themselves or standard traction force microscopy.^[73] In traction force microscopy (TFM), the displacement field of beads in the elastic substrate is used to calculate traction forces, usually by solving the inverse problem of elasticity theory. Length measurements of the deformed micropatterns can be performed in a high-throughput manner, but the dependence between force and length change depends on the geometry of the micropattern and must be calibrated with standard traction force experiments.^[72] Micropatterns can also be used to control the actin cytoskeleton network, specifically the growth of stress fibers, allowing for reproducible settings and the measurement of traction forces after photoablation of stress fibers.^[74]

Another method to measure cellular forces in well-controlled elastic environments are micropillar arrays, see **Figure 1f,f'**. These are uniformly distributed cantilevers of equal size typically made of polymer material such as PDMS and can be used as a rationally designed mechanical environment in single cell experiments.^[59,75] Compared to micropatterns, cells subjected to micropillar environment have larger variations in cell shape.

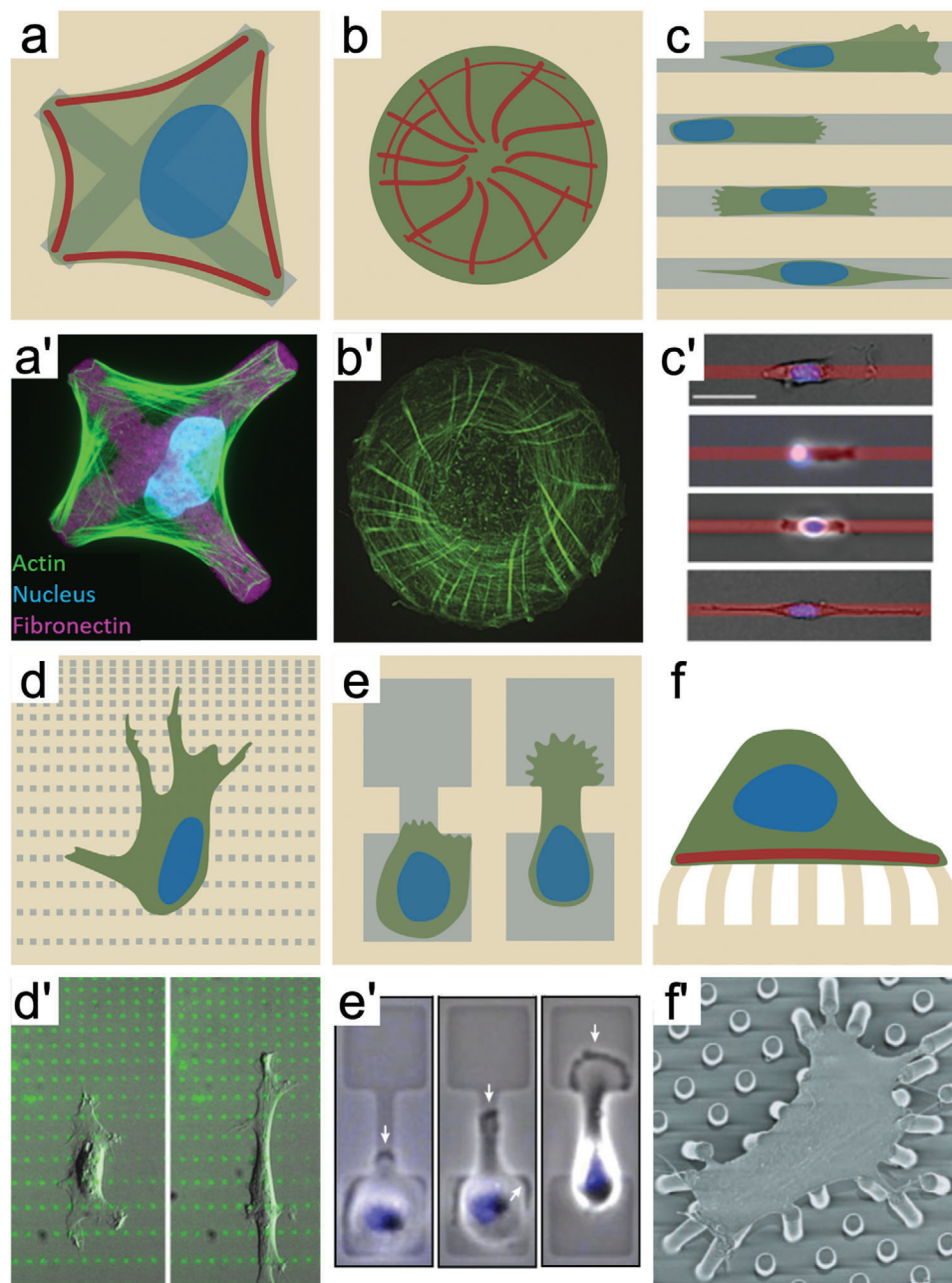


Figure 1. 2D environments for single cell experiments. a,a') Schematics (a) of a single cell on a cross pattern with nucleus (blue) and stress fibers (red), experimental image (a') stained for actin (green), nucleus (blue), and fibronectin (magenta). b,b') Schematics (b) and experimental image (b') of a single cell on a circular micropattern with different types of stress fibers. c,c') Schematics (c) and experimental images (c') of a human skin fibroblast (top row), human mesenchymal stem cell (second row), human malignant melanoma (third row), and murine fibroblast (bottom row) on fibronectin tracks. d,d') Schematics (d) and experimental images (d') of a single fibroblast cell on a substrate with discrete fibronectin sites of varying density. e,e') Schematics (e) and experimental images (e') of a single cell on a two-state pattern. f,f') Schematics (f) and experimental image (f') of a single cell on micropillars. Figure 1b': Reproduced with permission.^[64] Copyright 2019, The Company of Biologists. Figure 1c': Reproduced with permission.^[66] Copyright 2012, Elsevier. Figure 1e': Reproduced with permission.^[67] Copyright 2019, Springer Nature. Figure 1f': Reproduced with permission,^[68] Copyright 2003, National Academy of Sciences, U.S.A.

A major disadvantage is that the topography leads to cell processes being sent into the space between the pillars. This can be avoided by passivating the pillar sides. Traction forces can be calculated from Euler–Bernoulli beam theory with corrections resulting from substrate warping.^[76,77]

Cellular force generation can also be artificially altered by interfering genetically, chemically, or optically with the cell cytoskeleton.^[78] One of the most exciting developments in this field is non-neuronal optogenetics. Here cells are genetically modified to make specific proteins light-sensitive, which can then

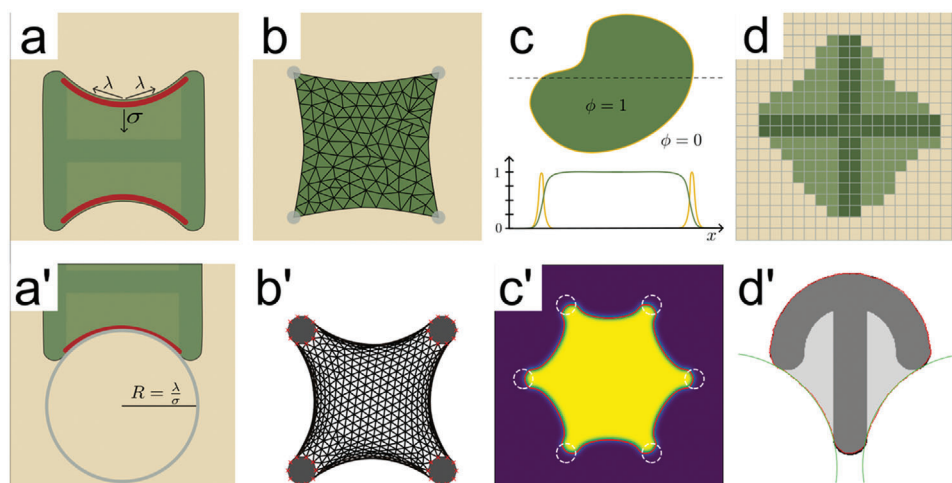


Figure 2. Models to describe cells in environments in 2D. a,a') Schematics of the contour model which predicts the radii of invaginated arcs from surface tension σ and line tension λ . b,b') Schematics (b) and image of a simulation (b') of a 2D network model. c,c') Schematics (c) and image of a simulation (c') of a 2D phase field model. d,d') Schematics (d) and image of a simulation (d') of a 2D cellular Potts model. Figure 2d': Reproduced with permission.^[91] Copyright 2014, Elsevier.

be targeted by light to, for example, contract actomyosin with a high spatiotemporal precision.^[79] Optogenetics as a tool to manipulate the cell cytoskeleton was first used to control cell migration of HeLa-cells by photoactivating Rac1.^[80] The design of optogenetic switches has proven a challenging task due to the complex feedback loops used by cells to control their cytoskeleton. An interesting approach is to combine optogenetics with adhesive micropatterning. For example, de Beco and colleagues investigated the gradient formation of Rac1 and Cdc42 during cell migration for single cells on circular micropatterns with optogenetic activation.^[81] Recently optogenetics has been used to revert cell migration in 1D situations.^[82,83] Optogenetics has also been combined with traction force microscopy to show that cell forces can be switched on and off by light.^[22,84] A recent combination with adhesive micropatterning revealed that cell size and actin architecture determine the dynamical response to such activation.^[85]

In addition to adhesive cues, cell behavior also depends on the curvature of the microenvironment, a process called “curvotaxis”. With initial observations that chicken heart fibroblasts on glass bars align along the minimal curvature line,^[86] it was later found by Pieuchot and colleagues that both fibroblasts and mesenchymal stem cells use their nucleus to measure the local curvature and migrate toward concave valleys.^[87] Werner and colleagues used stereolithography to manufacture concave and convex hemispheres for cells to adhere to.^[88] Mesenchymal stem cells increase their migration speed in concave environments, whereas cells in convex environments experience higher forces on their nucleus, which influences cell differentiation. For a detailed review on curvotaxis we refer to the work of Callens and colleagues.^[39]

2.3. Modeling Single Cells in 2D Structured Environments

The shape and forces of single cells have been modeled in two dimensions with a variety of different methods, including static contour models, network models, and continuum models as well

as dynamic models such as phase field models and the cellular Potts model.^[27,89,90]

Contour models describe the static boundaries of a sessile cell based on the idea that non-motile cells on substrates are effectively 2D and span their contours between focal adhesions, see **Figure 2a,a'**. They are strongly motivated by experiments with cells in structured environments, which often show strong geometrical features, compare Figure 1a. The simplest approach is to assume a constant surface tension σ , due to the contracting actomyosin cortex, and a constant line tension λ , arising from actin stress fibers lining the periphery and counteracting the cortical tension. The surface tension acts in the normal direction of the cell boundary, while the line tension is parallel to the boundary. A force balance then leads to a Laplace law $R = \lambda/\sigma$ describing the radius of invaginated arcs between adhesive points.^[92] This simple argument suggests a constant invagination radius. Experimentally, a linear relation between radius and spanning distance of invaginated arcs was found. This can be explained with the introduction of an additional elastic line tension^[93] or with a dynamical version of the interplay between tension and elasticity.^[94] Recently, elliptical arcs have been described for the case when the stress fibers do not line the periphery, but pull toward the cell body.^[95] Contour models can often be solved analytically and the dependance of input parameters on the solution as well as their biological meaning follow directly from the model. For example, they have been used to predict cell forces from shape.^[92] However, they have been devised mainly to describe cell shape on 2D adhesive micropatterns and cannot be easily generalized to different situations. Moreover, they use phenomenological effective model parameters such as surface and line tensions.

Network models describe cells as a 2D network of cables, thereby replacing the coarse-grained surface tension in contour models with a more detailed model that is directly motivated by the key physical properties of the actin cytoskeleton, see Figure 2b,b'. Actively contractile cable networks under isometric tension reproduce the experimentally observed invaginated arcs, independent of the architecture of the cable network,

revealing a fundamental and unconventional property of the contractile actin cytoskeleton.^[96] Therefore network models allow for the modeling of experimentally more complex situations, such as cells on micropatterns that are contracting due to optogenetic activation.^[22] Recently cable networks have been used to describe the effect of laser cutting stress fibers that are strongly connected to the actomyosin cortex.^[74]

Following more traditional approaches from continuum mechanics, cells in 2D can also be modeled as homogeneous 2D elastic sheets under tension.^[85,97,98] They assume the existence of intracellular stress and strain tensors, which are related linearly by a stiffness tensor. An additional active stress is introduced to describe the actomyosin contractile network, similar to active gel theory.^[99] The adhesion to the substrate is either modeled with a fixed boundary condition or with elastic springs (elastic foundation) representing sites of adhesion to compliant material. Finite element simulations can then be used to predict traction forces and stress distribution inside the cell.^[100] Continuum models are helpful to understand how processes at the boundaries propagate into cells and to predict cell forces on the scale of the whole cell.

In many situations of interest, a more dynamical description is desired than provided by continuum mechanics models, especially in the case of large deformations or even topology changes. Phase field models^[101,102] use an energy-based description, in contrast to the previous models, which are force-based. Energy-based models are better suited to describe and predict dynamics, but make it difficult to predict forces. In phase field models, an auxiliary field is used to represent the boundary of a cell, see Figure 2c,c'. Single cell migration can then be modeled through an energy functional with an additional polarization vector or velocity field to model cell motility.^[101,103]

A computationally very efficient alternative to phase field models is the cellular Potts model (CPM), which was initially devised to model cell collectives.^[104–107] Like phase field models, the CPM is an energy-based description of cells on a lattice, see Figure 2d,d'. A generalized cell represents a biological cell, a sub-cellular compartment, the surrounding medium, or other physical entities and can span over more than one pixel on the lattice. For 2D systems, the Hamiltonian typically consists of an elastic area constraint and interaction energies between neighboring pixels that belong to different generalized cells.^[108] In the context of cells on micropatterns, an alternative approach is the use of energy terms of area and line tension, combined with an energy gain for the occupation of predefined adhesive sites.^[91,109] Then area is not determined by the area constraint, but by the size of the adhesive area, reflecting the fact that cells in 2D can generate area by material transfer from 3D to 2D. In any version of the CPM, a modified Metropolis algorithm is used to find the energy minimum, making this approach essentially a Monte Carlo simulation. This is a very versatile framework that can be applied to model complex systems, however, some parameters used in cellular Potts type simulations do not have a direct biological interpretation.

2.4. Single Cells in 3D Structured Environments

In vivo, cells live in a 3D environment, and the difference between a 2D and a 3D environment can be sensed by cells.^[110,111]

Traditionally, the majority of single cell experiments were performed on stiff glass or plastic substrates, and the shift to include the 3D mechanical environment in the design of cell experiments only started in the 2000s.^[112] The shift from 2D to 3D environments was made possible due to advances in materials science and imaging, however, identifying the relevant mechanical factors in the local cell environment is more challenging than in 2D.^[113] Cells in 2D versus 3D environments show differences not only in internal organization and morphology,^[110,114] but also in cell migration,^[115] adhesion,^[116] and mechanotransduction.^[117] There are many approaches to investigate cell fate and behavior in 3D environments, including the use of 3D hydrogels^[46,118] or 3D-printed microfluidic devices.^[119]

Cells in 3D hydrogels, in particular the physiologically most important case of collagen gels, interact with their surroundings in a more distributed manner than in 2D, see Figure 3a,a', and this difference influences cellular mechanosensing, migration, and growth.^[120] As seen in Figure 3a, cell shapes in 3D collagen gels also show the invaginated arcs found for cells on adhesive micropatterns (compare Figures 1a and 2a), because the same competition between cortical surface tension and line tension in the contour is at play in 3D as in 2D.^[94,121] Similar to 2D traction force microscopy, beads can be placed in the hydrogel to measure the displacement and use it to calculate the forces exerted by the cell, but the technical challenges are much larger in 3D than in 2D, due to the required 3D imaging and the complicated mechanical properties of the 3D gels, which necessarily have to be porous to allow for nutrient supply.^[122] A different approach to using hydrogels to observe cellular force sensing is to spatiotemporally change the hydrogel stiffness with light and to observe cellular reactions to stiffness changes.^[123] Some 3D hydrogels, for example alginate, can also be manufactured with 3D printing, allowing for printed microvascular environments.^[124,125] Micro- and nano-contact printing can also be used in combination with some hydrogels such as PAA. Tabdanov and colleagues^[126] contact printed nano lines onto PAA hydrogels and showed that both actin and microtubule network architecture differed between in-groove and on-ridge regions. Similar scaffolds have been used as a platform to improve T cell migration in 3D, by both pharmacologically and genetically manipulating the microtubule-tractility axis.^[127]

Cells need space and nutrients to survive in 3D environments, and rather than using the porosity of the 3D matrix, one can generate compartments for cell culture within the matrix. Minc and colleagues placed single sea urchin eggs into PDMS microfabricated chambers and observed the cell division axis relative to the shape of the chamber, see Figure 3b,b'.^[128] In general, eggs from marine organisms are a very useful model system because they interact little with their environment and are very large, thus providing good imaging conditions. The cavities with different geometries have the same volume as the eggs, which are forced into a given cavity geometry with a coverslip, see Figure 3b. This study showed that the microtubule cytoskeleton positions the nucleus at the center and the division axis can be predicted by minimizing the microtubule force and torque in the cell.^[128] Actin polymerization, the formation of focal adhesions, and actomyosin contractility is also affected by geometrical constraints. Bao and colleagues controlled the size and shape of human mesenchymal stem cells in different 3D cavity geometries and sizes and showed

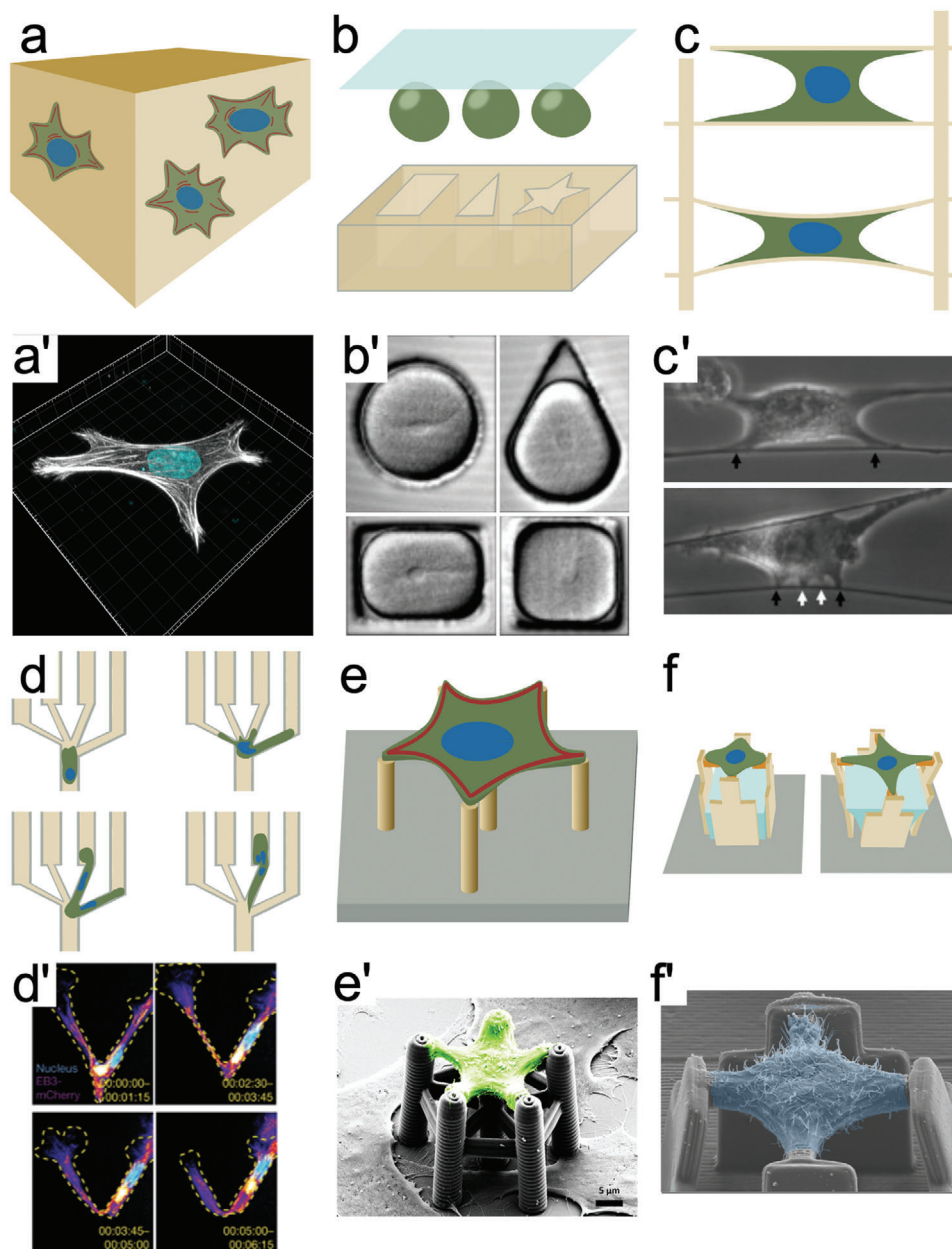


Figure 3. 3D environments for single cell experiments. a,a') Schematics (a) of single cells in hydrogel and experimental image (a') of a single cell in 3D collagen. b,b') Schematics (b) and experimental images (b') of sea urchin eggs in microfabricated chambers. c,c') Schematics (c) and experimental images (c') of single cells in nanonet structures. d,d') Schematics (d) and experimental images (d') of a dendritic cell in a channel with varying pore sizes. e,e') Schematics (e) and experimental image (e') of a single cell in a structure manufactured with direct laser writing. f,f') Schematics (f) and experimental image (f') of a single cell in a 3D microcylinder with a reversible host-guest system that can dynamically move the plates. Figure 3b': Reproduced with permission.^[128] Copyright 2011, Elsevier. Figure 3c': Reproduced with permission.^[129] 2016, Elsevier. Figure 3d': Reproduced with permission.^[33] Copyright 2019, Springer Nature.

that stress fiber density and distribution depend on both cell volume and shape.^[130]

A versatile method to mimic the mesh-like structure of the 3D extracellular matrix (ECM) is electrospinning of polymer/protein nanofibers.^[131] To date, nanofibers based on silk proteins,^[132,133] collagen,^[134,135] and gelatin^[136] have been used for various applications, including wound healing and tissue engineering.^[137–139] Although naturally occurring protein

nanofibers do not need any additional crosslinkers, the Young's modulus of polymer/protein nanofibers can be controlled either by adding bifunctional crosslinkers^[140] or by modifying the side chains by photocrosslinkers.^[141] Inspired by biological systems, crosslinker-free nanofiber materials have also been designed.^[142,143] It is well established that the elasticity (Young's modulus) of fibrous ECM is dynamically modulated during diseases and development. To model dynamic changes in fiber

elasticity accompanied with ECM remodeling, Hayashi and colleagues developed a gelatin-based nanofiber system that can modulate the Young's modulus by using reversible host-guest crosslinkers.^[144] Methods to fabricate 2D meshes can also be used to manufacture 3D structures, for example, by combining electrospinning with 3D printing^[145] or by placing the syringe on a freely moveable platform.^[146] 3D scaffolds produced with electrospinning are used to increase cell growth and viability for tissue engineering applications.^[131] Nain and colleagues advanced the electrospinning method to enable a precise manufacturing of micro- or nanofiber thickness and position with the spinneret-based tunable engineered parameters (STEP) technique, see Figure 3c,c'.^[147] Scaffolds produced with the STEP technique are called nanonets and can be used to measure mechanical forces and test the single cell response to external forces.^[129] When cells are seeded on the fibrous scaffold, they test their environment by pulling on the fibers. Again, one nicely sees the invaginated arc morphology resulting from the interplay of the different types of tension. From the displacement of the fibers, one can then calculate the forces exerted by the cell. With the use of a micropipette puller, one can also pull on a nanofiber that the cell is attached to and measure the adhesion forces of the cell.^[129] By changing the spacing between fibers within a scaffold, Jana and colleagues recently showed that the morphology and migration behavior of single cells strongly depends on fiber density.^[148] Cells on dense networks are elongated and have longer persistence lengths than on intermediate and wide networks.

3D structured environments can also be used to study cell migration in more physiological environments. Renkawitz and colleagues engineered a channel system to guide amoeboid cells, specifically dendritic cells, to a decision point, from which pores with width between 2 and 5 μm pan out,^[33] see Figure 3d,d'. Amoeboid cells typically migrate with the microtubule organizing center (MTOC) behind the nucleus, while mesenchymal cells usually have the MTOC and the Golgi apparatus in front of the nucleus. They demonstrated that the nucleus of dendritic cells in the channel is drastically deformed and protrudes into several pores before the cell proceeds into one of them. Decoupling the decision point from the constriction of the pore leads to a loss of pore-size preference, showing that the cells use their nucleus to measure the pore sizes. This explains why it is useful for amoeboid cells to migrate nucleus-first: it allows for a fast probing of the environment and a quick decision making.^[33] Using 3D nanofiber-based matrix with different degrees of crosslinks and tunable porosities, Huang and colleagues demonstrated that cancer cells invasively migrate into nanofiber stacks, while non-tumorigenic cells do not.^[149]

Traditional micropatterning requires the use of masks and is very time-consuming. This promises to be revolutionized by 3D additive manufacturing methods. The use of scaffolds manufactured with direct laser writing (3D nanoprinting), see Figure 3e,e', has the great advantages of allowing for rationally designed 3D environments as well as a high reproducibility.^[150] In 3D nanoprinting, a femtosecond-pulsed laser beam is used to excite photopolymerizable resists. Given the pulsed nature of the laser beam, two-photon polymerization is achieved, allowing to precisely polymerize material only in the focal voxel of the laser. By moving the laser focus along predefined trajectories, complex 3D structures with nano-resolution can be fabricated. With the

use of two different polymers, selected parts of the printed structures can be made adhesive, which gives additional possibilities for the scaffold design.^[23,121]

Similar to nanonets, structures manufactured with 3D nanoprinting can be used to measure forces of single cells positioned on beam-type structures. Klein and colleagues used chicken primary cardiomyocytes, which start contracting after 1–2 days after seeding onto the structure.^[151] The deformations of the 3D printed beams were measured and used to calculate the forces exerted by the cells. 3D structures fabricated with direct laser writing were also used to compare the volume of nuclei and cells in 2D and 3D environments.^[152] Fibroblast-like cells have a larger volume and nuclei in 3D compared to 2D environments, while there was no significant difference for epithelial-like cells. With the use of different photoresists, structures were deformable or non-deformable for cells. The soft and stiff 3D environment did not change the cell volume significantly.^[152]

3D structured environments fabricated with 3D nanoprinting improved cardiomyocyte derivation from pluripotent stem cells.^[153] 3D rectangular and hexagonal scaffolds were used to both constrain single stem cells geometrically and as contact points for cell attachment. The rectangular shape led to parallel alignment of myofibrils and an improved Ca^{2+} reuptake.^[153] 3D nanoprinting is also suitable to manufacture systematically varying sizes and shapes of so-called 2.5D microwells, which are open on the top side to allow cells to spread inside the chamber. By changing only a few parameters such as size and shape, the effects of these parameters on single cells can be observed in experiments. These structures were used to investigate the mechanotransduction via the yes-associated protein (YAP) in mouse embryonic stem cells.^[154] While the cell division rate increases for increasing adhesive area on 2D substrates, it decreases with increasing well size in 2.5D.^[154] More recently, Hippler and colleagues introduced a stimuli-responsive host-guest system, see Figure 3f,f, to measure cellular forces during cell stretching using structures fabricated with direct laser writing,^[155] see Figure 3f. With this host-guest system, cells can be stretched in a well-defined temporal and special manner. An advantage of this technique is that cells can be chemically fixed at any point during the experiment, allowing for a comparison of the actin cytoskeleton during and after stretching.^[155]

2.5. Modeling Single Cells in 3D Environments

In addition to new experimental methods, 3D computer simulations have increasingly helped to deepen our understanding of single cell mechanobiology in structured environments. Many previously described 2D simulation methods can be extended to three dimensions. For example, the shape of single cells 3D-printed scaffolds was described with a network model of active cables by Brand and colleagues, see Figure 4a,a'.^[121] The total energy is minimized numerically for a shape connecting the given adhesion platforms. They reported good agreement between the experimentally observed shape of a NIH 3T3 fibroblast and found the same curvature radius to spanning distance dependence as in the 2D contour model, although no explicit line tension was included. This suggests that the stress fibers lining the invaginations

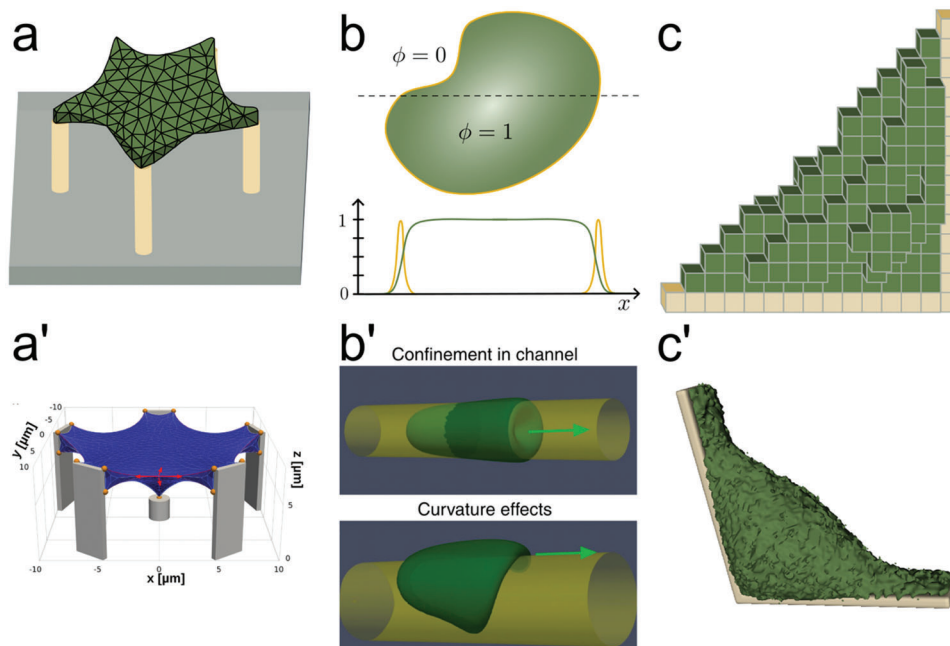


Figure 4. 3D models to describe single cells in environments. a), a') Schematics (a) and image from the network model simulation (a') of a single cell in a 3D structure. b), b') Schematics (b) and image (b') of a 3D phase field simulation. c), c') Schematics (c) and image (c') of a single cell in a 3D cellular Potts model simulation. Figure 4a': Reproduced with permission.^[121] Copyright 2017, Elsevier. Figure 4b': Reproduced with permission.^[156] Copyright 2019, Springer Nature.

in 2D are condensed versions of the actin cortex which is folding back onto itself in 3D.

Continuum models can be extended to three dimensions as well and are often implemented with the finite element method (FEM).^[157] Stiffness and viscosity of single cells or subcellular compartments can be measured and directly used as parameters in the simulations. Finite element models such as Cytosim^[158] have been used to describe crawling fibroblast and keratocyte motility.^[159] In addition to cell migration, 3D finite element modeling can be used to predict cellular responses of nanoindentation^[160] and to calculate the force distributions within cells.^[161,162] The open-source software Virtual Cell uses finite volume solvers to describe actin polymerization inside a 3D cell with a predefined geometry.^[163] Cytosim is an open-source software that can describe the mechanics of cytoskeletal networks using Brownian dynamics of fibers and motors.^[164] More coarse-grained models describe the formation of pseudopodia of a 3D cell on a 2D substrate with a finite element model^[158,165] or as an active nematic droplet.^[166]

Winkler and colleagues described single cells in 3D mechanical environments with an extended phase field model, see Figure 4b,b'.^[156] Both the cell and the mechanical environment are described with a scalar 3D field, while the actin inside the cell field is described with a vector field. The actin distribution inside the cell is modeled via a source term modeling actin polymerization close to the boundary, a sink term, and a diffusive term. Symmetry-breaking leads to front-read polarity and cell movement. This method predicts cell shape, velocity, and alignment on arbitrarily shaped substrates.

Extending the CPM to 3D is straight-forward, see Figure 4c,c'. Typically, the Hamiltonian includes an area constraint and a vol-

ume constraint, in addition to the interaction energies between neighboring generalized cells. Moreover, the nucleus can be implemented as a sub-cellular compartment with higher stiffness than the cytosol. Scianna and colleagues investigated the influence of a fibrous environment on a single cell with an explicit nucleus representation and compared cell velocity and persistence length for increasingly aligned fibrous networks and different pore sizes.^[167] More recently, single cell motion was described with the CPM by explicitly modeling lamellipodia of mesenchymal cells^[168] or by coupling the actin dynamics inside the cell to its shape and external cues.^[169]

The aim of many in silico experiments is to better understand cell migration in 3D.^[170] Predicting the 3D shape of a single cell in structured environments with the goal of improving scaffold design for biomedical applications is a novel research avenue and so far has only been discussed in 2D.^[171]

3. Cell Collectives and Monolayers

Tissue function requires not only the spatiotemporal regulation of subcellular structures, but also a coordinated cellular behavior across scales.^[172] Tissues are composite materials comprising different cell types and the extracellular matrix, which in turn is composed of three classes of macromolecules: collagens, proteoglycans, and non-collagenous glycoproteins. From a materials perspective, collagens resist tensile stress and proteoglycans resist compressive strain, while glycoproteins mainly serve as a type of glue by presenting binding sites for the cells.^[173,174] Individual cells in the tissue are mechanically linked together via different classes of cell-cell adhesions, mediated mainly by the cadherin superfamily,^[175] or indirect via cell-ECM adhesions, mediated

by the integrin family.^[176] Intracellular adaptor proteins and linker molecules connect these transmembrane anchors with the cytoskeleton, most notably actin filaments and intermediate filaments.^[177,178] Due to this network architecture, tissues exhibit far more complex mechanical behaviors than linearly elastic materials, including viscoelasticity, nonlinear elasticity, and mechanical plasticity.^[179,180]

Tissues have to cope with a large range of mechanical challenges. During development and regeneration, spatial patterns of cell growth^[181,182] or contraction of adjacent tissues^[183] can generate mechanical stresses that expand, push, bend, fold, and twist distinct cell populations into specific 3D forms.^[57,184] For example, one strategy to build an organism in 3D is to first build a 2D cell layer which then can be folded. The best-known case is the fruit fly, which forms a cell monolayer through its first 14 divisions that then is folded during gastrulation. In general, mechanical processes such as folding or buckling lead to complex folded and branched structures in our organs, such as in the lung, kidney, brain, intestines, or circulatory system.^[185] The remarkable degree of self-organization, cooperation, and synchronization across individual cells in a multicellular mechanical network has led to the paradigm that certain cell collectives behave as higher-ordered “supracells”.^[186–189] Spatial induction of fate-determinants,^[190,191] nonlinear interactions between individual cells or the ECM,^[192,193] and cell-to-cell variability^[194,195] enable symmetry breaking and pattern formation from a previously unspecified and homogenous population of cells. Although the induction of pattern formation is to a certain degree genetically encoded,^[196–198] full engagement and reinforcement of heterogenous cell patterning requires implementation of multicellular forces and compartment boundaries from the ECM.^[199–201] In certain cases, mechanics might be even equally important. Palmquist and colleagues found that mesenchymal mechanics are sufficient to spontaneously shape the regular morphological pattern of feather follicles in the skin of chicken embryos *ex vivo* and in the absence of fate-determining molecular programs.^[202,203] Similarly, Cohen and colleagues showed that the development of a periodic checkerboard-like pattern of hair cells and supporting cells in the mammalian hearing organ of Corti is based on mechanical forces rather than signaling events, as global shear and local repulsion forces on hair cells were sufficient to drive the transition from disordered to ordered cellular pattern.^[204] Thus, investigating the bi-directional influence of ECM geometry and tissue morphology in rationally designed cell culture environments bears the potential to dissect complex morphogenetic processes during tissue formation in simplified and controllable *in vitro* systems.

In contrast to single cells, cell collectives have a stronger power to change their environment, which then can feed back onto them. To permanently shape tissues during developmental and regenerative processes, cells have to structurally reorganize the surrounding ECM by degrading, realigning, or secreting new ECM molecules, processes that typically occur on the time scale of hours to months.^[205] These processes are often triggered or modulated by mechanical stresses that result from cellular growth and the subsequent increase in surface, volume and density.^[57] The structure of the surrounding ECM *vice versa* influences the induction and magnitude of multicellular mechanical stresses. With today’s abilities in microfabrication,

engineered cell culture substrates can address many aspects in this regard, by tuning the rigidity of the substrate, by patterning or shaping the size of the adhesive domains, or by including repulsive areas and physical barriers in the substrate.^[2]

3.1. Cell Collectives on Elastic Substrates

For cell collectives, elastic substrates have revealed many surprising processes that would have gone unnoticed otherwise. The most studied model system for collective migration is sheets of epithelial cells migrating into open space after removal of a confining barrier. This assay has been developed as a version of the traditional wound healing assay, but avoids the damage afflicted by the traditional scratching approach.^[206] When combined with elastic substrates, it allows to perform traction force microscopy and even to reconstruct stresses inside the cell sheets (using an approach called monolayer stress microscopy, MSM).^[207,208] Using TFM and MSM on soft elastic substrates, it has been shown that higher substrate stiffness correlates with increased collective migration speed, persistence, directionality, and coordination of epithelial monolayers, due to stiffness sensing at the edge of the cell colony and force transmission between cell-cell contacts.^[209] Sunyer and colleagues went one step further and used fibronectin-coated PAA-hydrogels with a stiffness gradient to show that sheets of epithelial cells are able to sense and collectively migrate toward the higher stiffness (durotaxis).^[111] While durotaxis has been described before for single cells,^[45] these experiments revealed that the collectiveness increased the durotactic sensitivity due to long-range intercellular force transmission in the colony, highlighting the supracellular aspect.^[11,210,211] A comparable behavior was observed for *Xenopus* neural crest cells (a multipotent mesenchymal cell population), which were shown to migrate in distinct clusters toward higher stiffness on PAA hydrogels.^[212] During migration, these clusters showed a higher-ordered supracellular behavior, with collectively coordinated actin polymerization at the migratory front and synchronous collective contraction at the clusters rear end.^[187] Strikingly, using *in vivo* atomic force microscopy, the group showed that the neural crest cells not only sense the gradient through cell-matrix adhesions, but also induce the gradient formation via N-cadherin mediated cell–cell interactions and softening of the adjacent placodes, thus self-generating the stiffness gradient on which they migrate *in vivo*.^[212] Importantly, these results are not restricted to stiffness gradients. When Clark and colleagues monitored the collective cell migration of human squamous cell carcinoma or colorectal carcinoma cell clusters on homogeneously elastic PAA gels coated with deformable collagen I networks, they found that the cells generated asymmetric collagen densities and alignments underneath the cluster, in the absence of any biochemical cue.^[213] Thus, the cells self-steer their migratory persistence by generating a viscoelastic gradient in the collagen fiber network.

The concept that cell collectives self-generate durotactic/mechanical gradients opens new directions that will shape our current understanding of how mechanoreciprocity between cells and the ECM steers collective cellular behavior during embryonic development, metastasis spreading, wound healing, and more.^[15,214–216] For example, it is a long-standing research

question with contrary results, how cancer cells interact with their stroma, which is often stiffer than comparable healthy tissue,^[217,218] while the cancer cells themselves tend to be softer,^[219] in order to collectively invade foreign tissue during metastasis formation.^[220] As this process requires detachment from the primary tumor site, intra- and extravasation of basement membranes, and collective migration through interstitial matrices, tumor collectives must breach several barriers and perform long-range migration through tissues with various stiffness. The stiffness of PDMS substrates was shown to promote epithelial-mesenchymal transition of MDCK cells, a process linked to cancer dissemination.^[221] However, it remains unclear how stiffness-induced malignancy is maintained over time after cancer cell dissemination *in vivo*. Self-generated gradients could allow cell collectives to operate over greater ranges of stiffness, larger distances, and longer times.^[222,223]

3.2. Cell Collectives in 2D Confining Environments

Like for single cells, 2D micropatterns are a very popular method to generate confining environments for cells, because microscopy is easy with planar substrates. Microcontact printing, photolithography techniques, or spotting-based molecular printing^[224] are among the most frequently used methods to transfer desired 2D shapes on coverslips or PDMS/PAA hydrogels.^[2,225] Raghavan and colleagues even developed a double microcontact printing approach to pattern gold-coated coverslips with self-assembled monolayers that include a region, which can be electrochemically switched from non-adhesive to adhesive, allowing to temporally control confinement release.^[226] Alternatively, large scale boundaries can be created via physical obstacles of a desired shape, which can be placed permanently or transiently via magnetic stencils.^[11] Transient application of a growth-restricting obstacle has the advantage that the confinement can be released at a defined time point, allowing to add the temporal dimension more easily.

As already mentioned above, 2D micropatterns with such confining barriers are very well suited to investigate different aspects of collective cell migration. As the adhesive area on which the cells are able to migrate can be rationally designed, it is possible to guide, restrict or coordinate the movement of the cell collective. These approaches replaced the classic “scratch assay” and allow to tackle fundamental questions of how cells generate distinct migration patterns in much more refined assays. Vishwakarma and colleagues used PAA hydrogels with a removable barrier to address the question of how leader cells are selected for their function in collectively migrating epithelial monolayers, and found that upon confinement release, leader cell territories emerge in response to force transmission from the follower cells.^[227] By designing stencils with different shapes, they showed that the distance between leader cells converges to a typical value $\approx 170 \mu\text{m}$ set by the mechanics of the cell monolayer. Vazquez and colleagues added a removable magnetic physical barrier with triangular cavities to a PDMS hydrogel, in order to spatially control the protrusion formation in the cellular monolayer.^[228] In another approach, pillar stencils have been used to fabricate microgaps of desired shape and size in epithelial monolayers.^[229] As the number, shape and size of the barrier stencil can be indi-

vidually shaped as desired, this approach is scalable and allows to simultaneously monitor gap closure along several spots, as a model for wound healing.

In contrast to wound healing assays, where cells move into an open space, micropatterns that restrict the migratory space can be used to guide the migratory cells along spatially defined routes, in order to monitor how spatial confinement affects the speed and directionality of migrating cell collectives. Vedula and colleagues^[230] as well as Marel and colleagues^[231] fabricated adhesive strips of different widths and monitored collective cell migration speed and persistence. Using particle image velocimetry, they found a negative correlation between the overall migration speed and the width of the adhesive strips.^[230] Other groups used confining patterns to monitor distinct motion patterns inside the cell colony. Peyret and colleagues showed that epithelial cells exhibit coherent oscillations when confined on micropatterns of varying shapes and sizes, with period and amplitude of the oscillations being dependent on the substrate size.^[232] Another advantage of this approach is that the size of the adhesive pattern can be adjusted, in order to tune the number of cells that are able to adhere to the substrate. Segerer and co-workers monitored the spontaneous formation of vortices on micropatterned circles, see **Figure 5a,a'**, and found that the persistence of coherent angular motion increased with the number of confined cells.^[233] Finally, asymmetries can be incorporated in the pattern, in order to guide collective cell polarization and migration.^[234] For instance, Rausch and colleagues plated cells on stencil-masks with varying local curvatures, see **Figure 5c,c'**. They showed that high curvature areas induce leader cell formation, and moreover that polarization of the cells and high traction forces in areas of high curvature even before migration.^[235] This growth guidance can in principle be mapped toward any desired 2D shape, from straight lines to branching points up to complex mazes, monitoring cellular path finding and decision-making branching morphogenesis.

Besides collective cell migration, 2D micropatterns have been proven valuable for ongoing research on how crowding and confinement affects cellular fate decision. As mentioned above, distinct patterns of cellular growth lead to different mechanical stresses at the edges of boundaries and in the center of the mass, respectively. It is an ongoing debate on how these different stresses affect cellular decision making. Depending on the cell type, different stresses might lead to the induction of differentiation, proliferation, or apoptosis, respectively. Nowadays, the flexibility in terms of shape and size of 2D micropatterns allows to precisely induce, guide, map, and monitor these stresses in cell colonies over time. Thus, micropatterned substrates are frequently used to decipher how different stresses are transduced on the molecular scale, in order to guide cell differentiation and cellular fate decision.

Gomez and colleagues showed that mouse mammary epithelial cells are under high mechanical stress along the edges of different substrate geometries that were printed on glass via microcontact printing and that these cells preferentially undergo epithelial-to-mesenchymal transition (EMT), while the cells in the center did not.^[236] Strikingly, inhibiting cytoskeletal tension abrogated the spatial patterning of EMT. In contrast, Wei and colleagues did not observe increased EMT, when they cultivated single MDCK epithelial cells on circular micropatterns.^[221] These results suggest that both multicellular confinement and the shape

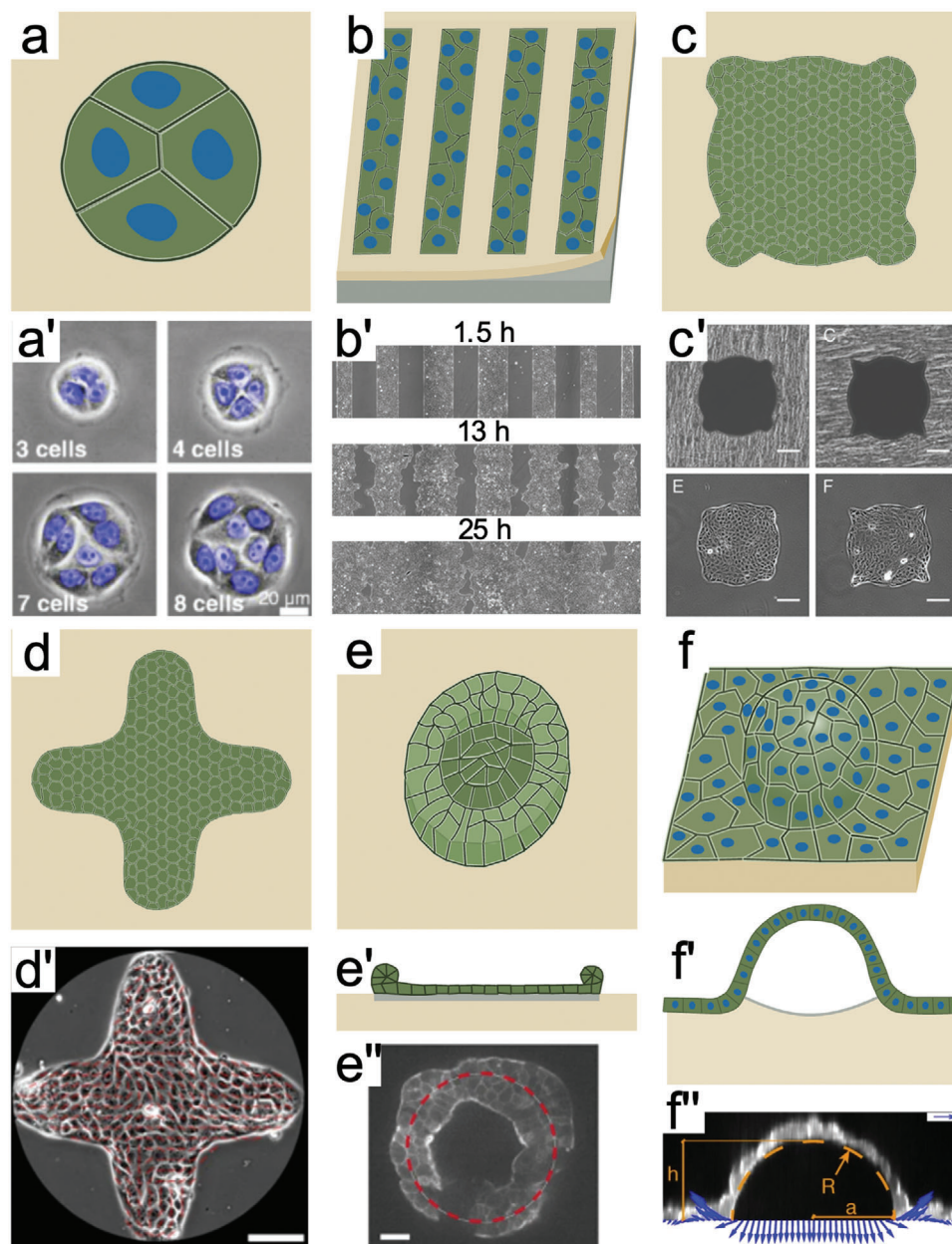


Figure 5. 2D environments for experiments with cell collectives. a,a') Schematics (a) and experimental images (a') of circular micropatterns to study collective cell migration. b,b') Schematics (b) and experimental images (b') of a wound healing assay with a removable microstencil. c,c') Schematics (c) and experimental images (c') of cell collectives on micropatterns to analyze the influence of geometry-based cues. d,d') Schematics (d) and experimental image (d') of microcontact printed cell monolayers to investigate cell extrusion. e–e'') Schematic top (e) and side (e'') view of adhesive cellular patterns to study monolayer development into the third dimension. e'') Experimental image of the ring region. f–f'') Schematic top (f) and side view (f') of epithelial cells seeded on soft PDMS substrate with micropatterned nonadhesive areas. f'') Experimental image of the side view and traction forces. Figure 5a': Reproduced with permission.^[233] Copyright 2015, American Physical Society. Figure 5b': Reproduced with permission.^[206] Copyright 2007, National Academy of Sciences, U.S.A. Figure 5c': Reproduced with permission.^[235] Copyright 2013, American Institute of Physics. Figure 5d': Reproduced with permission.^[240] Copyright 2017, Springer Nature. Figure 5e'': Reproduced with permission.^[241] Copyright 2014, Springer Nature. Figure 5f'': Reproduced with permission.^[242] Copyright 2018, Springer Nature.

of the geometric boundaries are important for the observed effects. This is in line with findings from Nelson and colleagues, showing that regions of concentrated growth corresponded to regions of high traction stress within a cell sheet on micropatterned substrates, while inhibiting actomyosin-based tension or

cadherin-mediated cell-cell connections disrupted the spatial pattern of proliferation.^[57] Similarly, researchers from the lab of Gregory Underhill fabricated elastic PAA hydrogels for traction force measurements and spatially deposited collagen in circular shapes onto the hydrogel via microcontact printing.^[237] Using this

approach, they found that liver progenitor cells exhibited patterned differentiation in response to spatially controlled downstream mechanotransduction. On the boundary, cells expressed high E-Cadherin levels and exerted higher traction forces, leading to increased biliary differentiation in this region, whereas cells in the interior differentiated toward the hepatocytic lineage.^[237,238]

These results clearly show that cell differentiation patterns arise from the mechanical status of distinct cell populations, which is in turn dependent on the ECM geometry and the boundaries. It should be the scope of future research to decipher the molecular downstream pathways that convert these mechanical signals into biochemical reactions. In this spirit, Muncie and colleagues cultivated human embryonic stem cell colonies on patterned hydrogels of soft nature (0.4–2.7 kPa) that recapitulate biophysical properties of the early embryo.^[239]

They found that specific geometries promoted local areas of high adhesion-mediated tension that enhanced spatial patterning of morphogens, ultimately inducing mesoderm specification. Of note, the clever integration of microfluidic devices in the hydrogels even allows to mechanically stretch the microtissues by controlling the pressure in the micropatterned compartments, leading to either negative or positive out-of-plane deformations of the epithelial monolayer.^[239,243] Using this approach, Blonski and colleagues showed that inward bending of the epithelium led to high tension in the adjacent cells next to the imposed negative curvature, inducing the spread of calcium waves, while positive curvature resulted in the opposite and prevented calcium spread.^[243] Thus, these studies demonstrate creative ways to combine soft elastic substrates, micropatterning, and active mechanical perturbation, in order to investigate the conversion of mechanical cues into biological patterning mechanisms.^[239]

Another interesting direction from the biophysical and biomechanical perspective is the transition from 2D to 3D growth due to confinement and cellular crowding. Given that cell proliferation in the restricted area leads to finite population size in 2D monolayers, cells react to this either by growth arrest or by cell extrusion, ultimately extending the growth in the axial direction and forming multilayered cell sheets. Saw and colleagues investigated cell extrusion in confined environments, see Figure 5d,d', and found that it is not cell density, but topological defects that lead to cell extrusion and apoptosis.^[240] Mechanically, folding or buckling is a sudden out-of-plane collapse of a material caused by an increasing in-plane compressive load.^[244] In order to monitor tissue folding and buckling in vitro, compression or confinement can be engineered by restricting the growth area of cells on the substrate.^[57,242,245] Deforet and colleagues monitored the latter process by confining cellular monolayers on circular micropatterns, see Figure 5e,e',e'', and found that cellular rims formed along the periphery of the substrate because of the additional degree of freedom of the border cells and independent of the substrate size.^[241] These results demonstrate that epithelial confinement alone can induce morphogenesis-like processes including spontaneous collective extrusion and transition from 2D to 3D.

Cell extrusion is not needed when the whole monolayer can escape into the third dimension to relax its growth stress. This process has recently been controlled using adhesive micropatterning. Latorre and colleagues cultivated an epithelial monolayer on adhesive PDMS gels that were interspersed with non-adhesive islands, see Figure 5f,f',f''. The cells eventually overgrew

the islands and formed pressurized cellular domes above these restrictive areas. The pressure within the domes was measured with 2.5D TFM. This experiment revealed the unusual elasticity of the cell monolayer, which showed strain values of up to 1000 percent, which until then has been known only for the “superelasticity” of metal alloys.^[242] Similar to the case of the metal alloys, these large strain rates are possible due to an underlying bistability in the system: first, the stress is held by the actin network, which then yields and gives way to a new stable situation provided by the intermediate filaments. Usually, tissues undergo small-scale deformations and the resulting changes are mainly elastic^[246] with a linear relationship between tensional increase and deformation.^[247,248] This allows cells in tissues to return to their default state after the stress is released, a process known as tensional or mechanical homeostasis.^[249,250] Above a certain threshold, however, the bonds between cytoskeletal filaments, cell-cell junctions, and cell-matrix adhesions rupture, leading to irreversible deformations that prevent full recovery, even if the associated stress is released.^[180,251,252] However, with the help of micro-patterned elastic substrates, Latorre and colleagues were able to provide an explanation of how certain epithelial tissues still can undergo reversible, large-scale elastic deformations in 3D, without tissue rupture.

3.3. Cell Collectives in 3D Confining Environments

As explained above, cell collectives in 2D often extend into 3D by themselves. However, today one can design assays that include the 3D aspect right from the start, in order to mimic the 3D physiological environment in vivo and to support and monitor collective supracellular growth in all three dimensions. Historically, in vitro pattern formation and higher-ordered supracellular behavior in 3D has been observed already in the early 1980s, in the context of connective tissue. In a reductionist approach, Stopak and Harris mixed fibroblasts and collagen to reconstitute connective tissue.^[253] To resist the collagen gel shrinkage, induced by the tensile forces from the fibroblasts, they simply attached fix points in form of polystyrene cylinders in the culture dish. Given that the free edges along the collagen-culture liquid interface served as a natural barrier, leaving nothing to attach, the fix points caused the cells to self-organize into aligned tracks along the margin of the collagen, in order to resist the centripetal stress, exerted by central cells. Around 25 years later, Bischofs and colleagues used a similar approach and found that the collective architecture of fibroblasts in collagen resembled the morphology of single fibroblasts on a macroscopic scale, if the boundaries, that is, the subcellular adhesion sites of the single fibroblasts and the anchor points of the hydrogel, are comparable in geometry.^[93] In both cases, the previously described relation of tension and elasticity leads to the observed phenotypes, however, the structural architecture arises on different scales. While bundled actin arcs restricted the edges of the single cells, the edges of the collagen hydrogel were defined by polarized cells that aligned perpendicular to the direction of the central stress, resembling the structure of individual actin arcs in the single cells on a supracellular scale. Although being an extreme example, this shows that cell collectives resemble certain biomechanical aspects of single cell morphogenesis, given that the geometric boundaries are predefined.

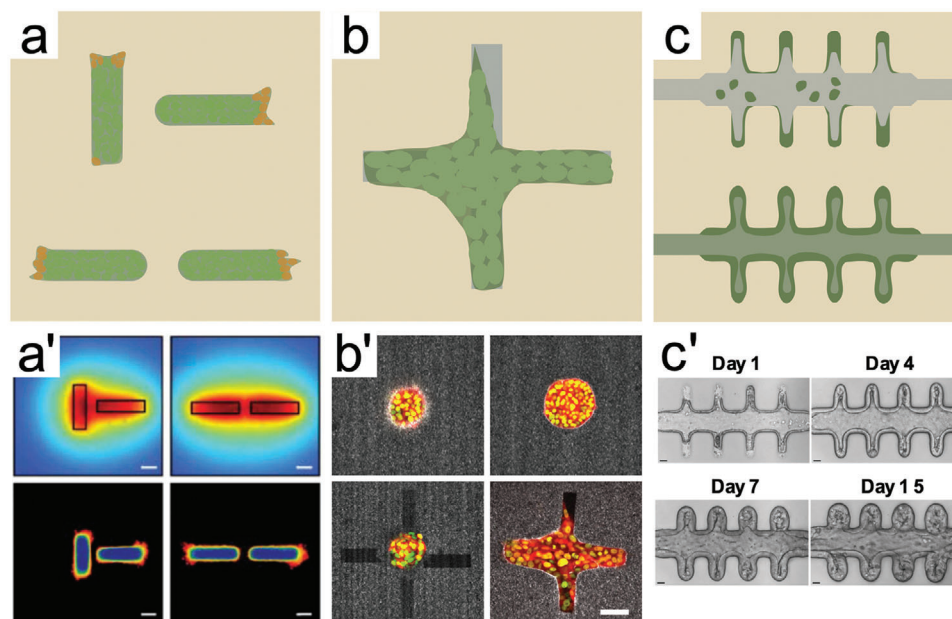


Figure 6. Experiments with cell collectives in 3D structured environments. a,a') Schematics (a) and experimental images (a') of epithelial cells growing in cavities of collagen gel. b,b') Schematics (b) and experimental images (b') of mammary tumor breast cancer cells in 3D microtracks of collagen matrices created with two-photon laser ablation. c,c') Schematics (c) and experimental images (c') of intestinal stem cells in a collagen microchannel generated with laser ablation. Figure 6a': Reproduced with permission.^[254] Copyright 2006, American Association for the Advancement of Science. Figure 6b': Reproduced with permission.^[255] Copyright 2011, IOP Publishing. Figure 6c': Reproduced with permission.^[256] Copyright 2020, Springer Nature.

Today modern microfabrication techniques like 3D nanoprinting enable researchers to engineer cell culture systems with physical boundaries down to the microscale. Multicellular force generation in such scaffolds can be monitored by state-of-the-art light microscopy in space and time, allowing to perform much more refined assays. To generate 3D microstructures with defined geometry, micro-molding or stenciling techniques have emerged as valuable tools. In principle, the same elastic polymers that are regularly used to fabricate plane 2D substrates can be used to cast desired 3D shapes from a master structure, that is, a positive replica of the desired form. Thus, the structures can be fabricated with different elasticities, optionally from synthetic polymers or from biologically-derived materials like collagen, and can be combined with TFM to estimate the cellular forces.^[254,257,258] Moreover, micro-molding processes are not restricted to soft materials, as components like ceramic powder can also be incorporated in polymerizable materials, to fabricate stiff scaffolds to promote, for example, osteogenic differentiation.^[259] However, due to the nature of the casting process, the incorporation of small topographies or fine details in the structure is difficult. Nevertheless, micro-molded 3D structures can be used to monitor tissue growth in a nutshell, and confinement in all three dimensions can be achieved by adding a lid on the micro-molded structure, see **Figure 6a,a'**.^[254]

Mechanobiological research in micro-molded 3D environments receives growing attention as advances in volumetric imaging and optical sectioning nowadays allow capturing large 3D stacks with increased axial resolution in a reasonable amount of time. This in turn allows to tackle long-standing basic questions, for example, if and how the mechanisms of collective cellular force generation differ between 2D and 3D setups. How-

ever, compared to plane 2D substrates, force calculation and mapping of cellular stresses is much more challenging. Gjorevski and colleagues micro-molded 3D collagen hydrogel structures of different geometries and incorporated fluorescent microspheres for the calculation of tissue stress within epithelia.^[257] To account for the heterogeneities in the collagen network, they performed confocal reflectance and AFM measurements. Together with computational modeling, these techniques allowed them to quantify patterns of mechanical stress throughout the surrounding matrix and to observe unexpected geometry-dependent mechanical behavior in curved duct-like tissues. The same approach was used to monitor the stress and pulling forces, exerted during collective cell migration, showing that tensile forces at the invasive front propel the colony forward and condition the cells and matrix for further extension.^[258]

Besides these basic mechanobiological questions, micro-molded 3D structures are used frequently to monitor biological and cellular output in response to the 3D environment. Similar to plane 2D micropatterns, studies investigating cell proliferation, differentiation, and collective cell migration are among the most prominent. Kollmannsberger and colleagues used microscope projection lithography and micro-molding to fabricate 3D PDMS scaffolds with macroscopic square-shaped clefts for the cultivation of microtissues.^[260] Using this set-up, they monitored microtissue formation over several weeks and found that especially at the highly tensed growth front, cell proliferation was up-regulated and fibroblasts transitioned into myofibroblasts. Thus, predicting tension generation in patterned tissues allowed to correlate multicellular forces and cell proliferation in 3D, similar to examples described in the 2D set-ups above. Similarly, Nelson and colleagues fabricated surfaces with pyramidal arrays and

found that cell proliferation was highest in the grooves, suggesting that the tissue form can feed back to regulate patterns of cell proliferation.^[57] Xi and colleagues monitored collective cell migration in 3D microchannels.^[261] Their experiments revealed emergent patterns of collective cell migration under tubular confinement: In contrast to flat constraint, cell sheets in smaller microtubes demonstrated slow motion with periodic relaxation, but fast overall movement in large microtubes.

The flexibility of photolithographic and soft-lithographic approaches allows to upscale the dimensions and complexity of the 3D structures, in order to steer multicellular growth on the scale of millimeters. The approach of Xi and colleagues, with cells crawling through microchannels, was designed to mimic tubulogenesis.^[261] Moreover, increasing the complexity of the structures can resolve cellular decision-making processes during tissue growth, for example, during vascularization and branching morphogenesis in glands and lung tissue. This was for instance done by monitoring the growth of epithelia in microchannels with different curvatures,^[262] resembling tissue folding and winding growth processes as they occur in the brain or in the intestine. Nelson and colleagues harvested this approach to control the initial 3D structure of mouse mammary epithelial tubules.^[254] By quantifying the extent of branching, they found that the geometry of tubules dictates the position of branches, as they initiated at sites with a local minimum of autocrine inhibitory morphogens, revealing that tissue geometry can control organ morphogenesis by defining the local cellular microenvironment.

Besides these micro-molding approaches, several other creative approaches have been established to investigate the multicellular behavior in complex 3D environments. To monitor collective cell invasion of completely encapsulated cancer spheroids in collagen hydrogels, Ilna and coworkers used an approach that does not rely on the pre-casting of microstructures, but rather on the generation of micro-tracks via two-photon laser microsurgery after cell seeding and hydrogel polymerization, see Figure 6b,b'.^[255] Using two-photon excitation, regions of interest with variable lengths, widths, and depths can be positioned directly adjacent to the edge of multicellular spheroids. This gives a striking degree of freedom, allowing not only to monitor invasion in real 3D confinement, but also to dynamically adjust the micro-tracks to the desired need. This laser ablation approach was also used to show that E-cadherin dependent cell-cell adhesion and extracellular matrix confinement cooperate to determine unjamming transitions and stepwise epithelial fluidization during breast cancer invasion.^[216] Nikolaev and colleagues laser-ablated a gut-like 3D structure in a hydrogel, see Figure 6c,c', and observed epithelium formation and cell-fate patterning in these environments.^[256]

Another way to increase the complexity of 3D scaffolds for cell cultivation was established by adapting 3D printing approaches toward biomedical research. On the multicellular scale, both bottom-up and top-down approaches are basically established to engineer cell patterning and microtissue formation. Extrusion-based, inkjet-based, and laser-assisted bioprinting is among the most common approaches to spatially deposit cell-laden bioink in complex 3D forms. Given the extent of this growing area of research, we refer to more comprehensive reviews for further reading.^[263,264] Trushko and colleagues recently developed

a different interesting bottom-up approach for mechanobiological applications.^[265] Using a 3D printed microfluidics device,^[266] they produced hollow alginate spheres with encapsulated epithelial cells in the center and Matrigel coating on the inner surface of the spheres. Upon reaching confluency in the monolayer grown on the inner side of the sphere, confinement leads to the local detachment from the Matrigel and folding of the sheet toward the sphere center.^[265] Considering the apparent pressure required for buckling together with a continuum theoretical approach, the authors established a minimal system to monitor stress-induced epithelial folding and conclude from these experiments that both capsule stiffness and cell stiffness have to be high, in order to relax excess cell proliferation by buckling.

In principle, such approaches can be refined down to the microscale by combining different techniques and additive manufacturing. As described above, 3D nanoprinting techniques allow to fabricate 3D structures in the regime of single microns and an increasing palette of available biocompatible photoresists with protein-adsorbing or protein-repellent features and tunable stiffness ranges, can be used to fabricate sophisticated scaffolds with complex geometry and topography landscapes.^[24,267] Published results in recent years show the biocompatibility of 3D printed micro-scaffolds with various cell types and populations under different conditions. For example, micro-scaffolds have been adapted to monitor and guide neurite outgrowth,^[268,269] microglia cultivation,^[270] or glioma cell colonization.^[271] Complex woodpile scaffolds were used to monitor cell invasion through narrow spaces in response to growth factors.^[272] The recent and rapid improvements in 3D nanofabrication, for example, the development of faster printing techniques,^[273,274] will allow to fabricate large-scale composite scaffolds for studies on microtissues in the near future.

3.4. Modeling Cell Collectives

Cells in collectives exhibit complex behavior such as collective migration and pattern formation that in principle could result from relatively simple rules being followed by the single cells. Thus, these are ideal model systems to be studied by mathematical and especially by computational models. As we have seen above, epithelial tissue is characterized by cell coordination over large length and time scales, resulting from mechanosensitive interaction between cells via cadherin-mediated adhesions.^[275] The strong cohesion in these systems means that modeling can proceed either by individual-based or continuum models. In individual-based models, cells are described by single or multiple particles, either in a continuous space or on a lattice. Cell activity resulting in motion can then be introduced by self-propulsion, like for active Brownian particles. Cell sheets can also be approximated as continuum elastic or fluid materials. Then cell activity resulting in motion is typically modeled by active stresses, which usually arise from actomyosin contractility.

Cell-cell interactions can easily be implemented in the cellular Potts model by including interaction energies between cells in the Hamiltonian. With the introduction of two cell types and the definition of pair-wise interaction energies, see Figure 7a,a', the differential adhesion hypothesis^[276] was implemented numerically in 2D as the first application of the cellular Potts model.^[277]

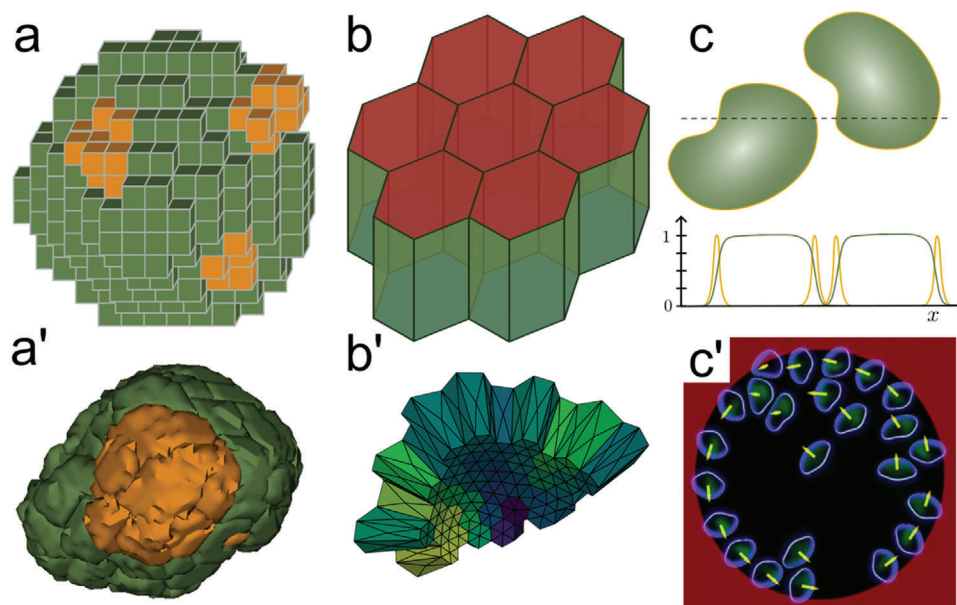


Figure 7. Models to describe cell collectives in structured environments. a,a') Schematics (a) and image (a') of a 3D Cellular Potts model describe cell sorting, a process where cell types arrange according to the difference in their adhesion strength. b,b') Schematics (b) and image (b') of a vertex model, describing tightly packed monolayers. c,c') Schematics (c) and image (c') of a phase field model simulation of interacting cells on an adhesive micropattern. Figure 7c': Reproduced with permission.^[282] Copyright 2015, Springer Nature.

Soon, it was extended to 3D and coupled with partial differential equations to describe chemotaxis, which allowed the modeling of the formation and crawling of *Dictyostelium discoideum*.^[105] This model has been adapted and extended by Merks and colleagues to describe vasculogenesis, where cell elongation was described explicitly with an additional energy contribution.^[106] More recent 2D simulations based on the cellular Potts framework focus on describing both single and collective cell dynamics.^[278,279] Due to its versatility, the cellular Potts model can be extended to 3D and applied to more complex systems, such as reproducing the morphology of vascular tumors, their growth, and angiogenesis.^[280]

In contrast to the cellular Potts model, which uses very variable cell shapes, the 2D vertex model uses simple polygons to describe epithelial monolayers.^[281] The forces acting on the vertices can result either from phenomenological laws or from an energy formulation as in the cellular Potts model. Using the purely geometrical Voronoi tessellation, which divides space into cellular compartments based on the neighborhood relations of their centers, one also can use a formulation that makes the system similar to individual-based models. Typical terms for the energy function include elastic constraints on the volume and area of the polygons, as well as an interaction term for neighboring polygons proportional to the length of the boundary interface.^[283] In 3D, one uses polyeders rather than polygons, see Figure 7b,b'. One of the first applications of the 3D vertex model was a simulation of the *Drosophila* wing disk, which showed that the tension in the system was sufficient for the formation of the dorsal appendages of *Drosophila* eggshells.^[284] The ensemble behavior of vertex models can be approximated with a continuous mean field theory. Czajkowski and colleagues developed a hydrodynamic model that takes cell shape anisotropy, motility, and po-

larization into account to model pattern formation in embryonic development.^[285]

The phase field model can also be used to describe cell collectives. In one of the first formulations of multicellular systems with the phase field model, each cell is modeled by a separate phase field, see Figure 7c,c', and the phenomenological free energy of the system includes term for the individual cell shape, the interaction of the cell with the substrate and with other cells.^[286] Löber and colleagues coupled the scalar phase field to a vector field describing the orientation of actin fibers inside the cell to model cell collisions.^[282] A different approach is to model a cell sheet as a single phase field. By adding elastic forces to the phase field equation, Chojowski and colleagues describe a reversible elastic phase field that captures deformations due to contractility and finger formation.^[287]

4. Organoids and Organotypic Cultures

One of the most exciting developments in modern biology are organoids, which are 3D cell assemblies that differentiate and grow in the test tube and thereby develop organ-/tissue-specific features.^[13,288] They are closely related to stem cell technology, because fate induction is typically achieved in induced pluripotent stem cells (iPSCs). Up to date, a wide range of organoid types from different cellular origins have been developed. This includes not only basic embryonic spheroids resembling early developmental stages, like blastuloids, gastruloids, or epithelial organoids, but also spheroids derived from adult stem cells that resemble specific organ types or sub-organ regions, for example, intestinal organoids, retinal organoids, or cerebral organoids. These features make organoids an attractive choice for basic biomedical research, for example, for in vitro drug testing on

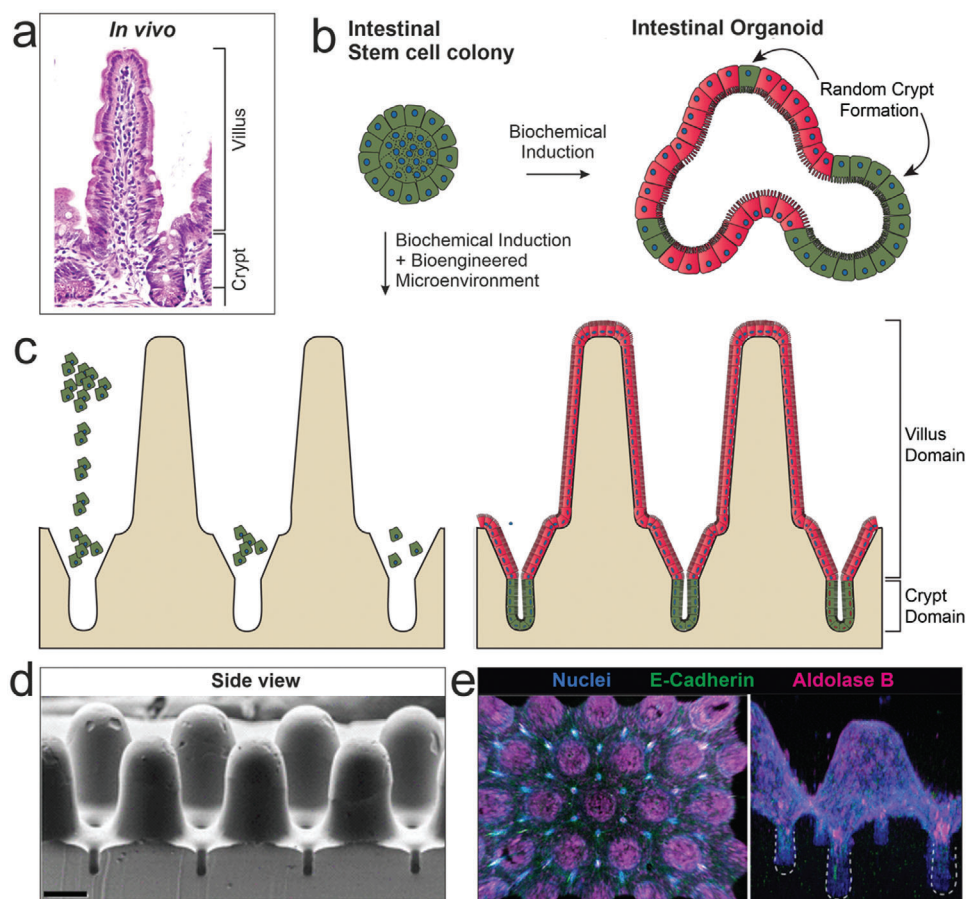


Figure 8. Self-organized versus directed growth of organoids. a) Immunohistochemical staining of the in vivo intestinal epithelium, showing the typical architecture with villus and crypt domains. b) Self-organized intestinal organoids can be derived through biochemical differentiation from isolated crypts or intestinal stem cells, but suffer from heterogeneities in size, morphology, and cellular composition. Crypt domains harbor the stem cells in intestinal organoids but form at random positions. c) Recapitulating the in vivo architecture of intestinal epithelia in biomimetic 3D scaffolds directs patterning of the different cellular domains. When seeding dispersed intestinal stem cells onto the scaffolds, they self-organize into villus- and crypt-like domains in response to the scaffold architecture. d) Scanning electron micrograph of a biomimetic 3D scaffold, recapitulating villus- and crypt domain architecture. e) Immunofluorescent staining of the same scaffolds after cellular colonization. 48 h after cell seeding, intestinal stem cells established a confluent monolayer. Induction of differentiation resulted in stereotyped organoid patterning. Aldolase-B (magenta) marks enterocytes and other differentiated intestinal cell types in the villus-domain, E-Cadherin (green) marks stem cells in the crypt domains. Figure 8a: Reproduced with permission.^[289] Copyright 2013, Elsevier. Figure 8d,e: Reproduced with permission.^[26] Copyright 2022, American Association for the Advancement of Science.

patient derived material or for the investigation of organ development processes in a simplified system. In the long-term, organoids might bear the potential to overcome some of the long-standing problems in regenerative medicine, as they in principle allow to differentiate organs-in-a-dish from patient-derived stem cells. However, major weaknesses of the organoid technology thus far are the lack of reproducibility and their heterogeneity in terms of ill-defined sizes, morphologies, patterning, cell type composition, and differentiation efficiency, thus so far limiting their application in clinical research.

The induction of organoids, that is, the activation of distinct fate programs in stem cells, requires not only the addition of certain biochemical factors, but also, at least equally important, embedding the cells in a 3D matrix, typically in cell-derived matrices like Matrigel. Due to the natural origin of these products, their biomolecular composition often varies significantly between different lot numbers and charges, leading to the above-mentioned

heterogeneities. Moreover, the self-organizing capacities of the organoids are limited, meaning that autonomous growth, folding, and differentiation processes only occur up to a certain degree, possibly because certain cues are missing that exist in a physiological context.

To narrow the gap between self-organizing organ development in vivo and organoid growth in vitro, microfabrication approaches that allow to generate defined 3D synthetic cell niches offer exciting possibilities. One of the best-studied (and most suitable) examples in this regard are intestinal organoids, see **Figure 8**. In vivo, the architecture of the small intestine can be subdivided into the functional units of villi and crypts, with the latter harboring a reservoir of intestinal stem cells (Figure 8a). Gjorevski and colleagues recapitulated this architecture in microscaffolds to improve the structure and reproducibility of intestinal organoids.^[26] In contrast to the randomized spatial induction of crypt domains under conventional culture conditions

(Figure 8b), cultivation in 3D microstructures instructed the precise cellular self-organization into crypt and villus domains, respectively (Figure 8c–e). Another approach used a collagen-based scaffold and achieved similar results,^[290] showing that indeed the 3D architecture of the scaffold is important to drive self-organization of intestinal organoids. Nikolaev and colleagues went another step further and bioengineered intestinal stem cells via scaffold-guided organoid morphogenesis into tube-shaped epithelia with an accessible lumen that was connected to a microfluidic system, see Figure 6c,c'.^[256] While the scaffold allows guiding organoid morphology toward an *in vivo*-like architecture, the perfusion system allows the continuous removal of metabolites and cellular debris, prolonging the microtissue lifespan to several weeks. This concept comprises another step toward functional organoids-on-a-chip.

Microfabricated scaffolds were also used to decipher the biomolecular mechanisms behind these morphogenetic processes. Using micro-molding and photopatterning, it was shown that the geometry-driven cell patterning in intestinal organoids arises from local differences in cell crowding that guide the downstream activity of the mechanosensitive transcriptional co-activator YAP.^[26] Regions of high curvature lead to increased cell crowding and YAP remains inactive in the cytoplasm, leading to the upregulation of intestinal stem cell markers. In less narrow and flat regions, YAP is imported into the nucleus and promotes intestinal stem cell differentiation into absorptive cells of the villus-like domain. In traditional organoid culture, this process acts stochastically and leads to random crypt formation in regions where curvature is generated by differential actomyosin contractility and luminal pressure.^[291,292] Again, soft elastic substrates helped to define the force distribution during these processes, unveiling how patterned forces enable compartmentalization, folding, and collective migration in the intestinal epithelium. Pérez-González and colleagues mapped 3D force distribution in mouse intestinal organoids, showing that the crypt shape relies on cell surface tension and cortical actomyosin density. Cells of the villus-like domains are subsequently dragged out of the crypt along a gradient of increasing tension.^[293]

In addition to investigating morphogenetic features of intestinal organoids on micropatterned 2D and 3D substrates, a range of different approaches start to control the formation of various organoid and organotypic tissues by tuning the respective culture substrates. **Table 1** summarizes some of the most frequently used cellular systems and approaches in recent research.^[292]

This list is just a glimpse of the long list of organogenetic processes that might be targeted in the future. Numerous developmental processes that lead to the formation of stratified and layered tissues rely on the reciprocal transduction of mechanical signals between the cells and the ECM^[310] and thus bear the potential to be manipulated/guided by microengineering approaches. Furthermore, the above-described knowledge might be included in future research and combined with larger-scale biofabrication and bioprinting approaches, for example, to guide the vascularization of growing organoids and to recapitulate complex architectures of vascular beds in biomimetic scaffolds.^[311–313] Current materials and microfabrication approach steadily increase our ability to mimic complex shapes and furthermore start to improve scaffolds for long-term cell cultivation, for example, by including dynamic dimensions like perfusion systems or con-

trolled release of molecules.^[314] Blatchley and colleagues recently provided a comprehensive review of various techniques for spatiotemporal regulation of organoids, including top-down methods such as extracellular matrices, bottom-up approaches such as confined environments to position single cells, and middle-out engineering, which utilizes external stimuli such as optogenetics to modulate both scaffold properties and cell behavior in time.^[14]

Organoids are complex interacting cell systems and combining them with structured environments is a promising novel approach. Again, mathematical and computational models might help to better understand how different cues interact with each other. To account for the complexity of cellular systems, simulations of organoids often include both biomechanical properties as well as signaling pathways.^[315] The optic cup formation of retina organoids was successfully described with a vertex model that includes cell growth and division, intercellular signaling, and cell shape deformations.^[316] These simulations suggest that mechanical feedback is important for formation of the optic cup.^[317] In addition, the vertex model was combined with a reaction-diffusion model for activation and inhibition to describe undulation, tubulation, and branching.^[318] Cerruti and colleagues used a cellular Potts model approach to simulate lumen formation in epithelial cysts, suggesting that accumulation of multiple lumens correlates with fast cell division rates.^[319]

While there are successful models of organoid morphogenesis^[317,320] and growth,^[321] these models typically do not include interactions with the extracellular environment. A first approach to include the local microenvironment in the mathematical model describes Matrigel as a semi-flexible elastic polymer network that gives rise to a bending rigidity of the organoid surface. The polymer network can be remodeled by the cells attached to it and the local curvature of the organoid surface partially regulates cell specification. This model describes intestinal spatiotemporal organization and growth.^[322,323] A continuum approach was used to better understand the oxygen transport and consumption in human midbrain organoids. Oxygen levels of an organoid in laminar flow were modeled with a reaction-diffusion model describing oxygen diffusion in the local microenvironment as well as diffusion and consumption in the organoid.^[324] In summary, theoretical approach can help to better understand the complex interplay between different aspects of cellular systems. Once established, it might also guide the design of future experimental systems and applications.

Some of the theory work presented in this review is summarized in **Table 2**. Moreover, an overview of the established physical models, their application area, advantages, and limitations are given in **Table 3**.

5. Conclusion

Cell culture is one of the most important achievements of the life sciences and allows us to perform systematic and quantitative experiments outside living organisms. The beginnings of *in vitro* cell culture were characterized by attempts to specify and improve cellular culture conditions via the use of chemical compounds, including growth factors, hormones, and cytokines. Customized culture media formulations were established that activate biochemical signal cascades promoting proliferation, differentiation, or simply survival of specific cell types. They were

Table 1. Summary of recently established approaches, combining engineered cell culture substrates and organoids or organotypic tissues. iPSC: induced pluripotent stem cell.

Study	Pattern/scaffold type	Cell/organoid type	Main finding
Neurulation and neural tube morphogenesis			
[294]	PEG-Hydrogel on an elastomeric membrane	Neural organoids derived from human iPSC	Stretching organoids in the hydrogels activates forces that guide their fate, patterning, and morphogenesis in 3D.
[295]	Micropatterned 2D substrates	Neural organoids derived from human iPSC	Controlling the initial tissue architecture is sufficient to polarize the arising neuroepithelial tissue.
[25]	Micropatterned 2D substrates	Neural organoids derived from human iPSC	The culture system precisely tunes morphogenesis in 3D. Organoids self-organize and fold into millimeter-long neural tubes covered with non-neural ectoderm.
Lumenogenesis			
[296]	3D micro-channels	Human iPSC colonies	The induced lumen can be shaped by the geometry of the micro-wells.
[297]	3D micro-wells	Hepatocytes	Symmetry breaking from hollow cysts is facilitated by anisotropic intercellular stress that guides lumen elongation in the direction of minimal tension.
Neurogenesis			
[298]	Micropatterned 2D substrates	Neuruloids derived human embryonic stem cells	The patterned substrate was used to engineer standardized human telencephalic neural rosettes, in order to model developmental aspects of Huntington's disease in the ectodermal compartment.
[299]	Floating PLGA fibrous microfilaments	Cerebral organoids derived from human iPSC	Scaffolds were used to engineer cerebral organoids with enhanced neuroectoderm formation, cortical development, and cortical tissue architecture, including formation of a polarized cortical plate and radial units.
[300]	Axially aligned 3D collagen scaffolds	Primary hippocampal neurons	Scaffold promoted the formation of 3D hippocampal neural circuits. CA3 neurons extended parallel axons and synapsed with CA1 neurons along the collagen fibers.
Osteogenesis			
[301]	Porous 3D collagen scaffolds with aligned pores of homogeneous size	Human bone marrow stem cells	Bone mimetic scaffolds promote cell patterning and vascularization during early wound healing.
[302]	3D-printed biomimetic bone scaffolds	Bone marrow mononuclear cells	3D-printed bone scaffold that mimics the trabecular architecture to monitor bone metastasis formation in vitro.
[303]	Macroporous 3D PEGDA hydrogel scaffolds	Hematopoietic stem cells/mesenchymal stem cells	Scaffolds mimic the trabecular architecture to serve as hematopoietic stem cell niche. Co-culture in the 3D scaffold showed a more pronounced preservation of hematopoietic stemness than in standard 2D cell culture systems.
Embryonic development			
[304]	3D patterned PEG hydrogel	E 3.5 mouse embryos (consisting of the inner cell mass and the trophectodermal cells)	Scaffolds mimic a uterus-like microenvironment to recapitulate mouse development ex vivo up to embryonic day 5.25.
[304]	Micropatterned 2D substrates	Human embryonic stem cells	Control of colony size is able to direct human embryonic stem cells fate to either the mesoderm or the endoderm lineage.
[305]	3D mesh-scaffolds	Human iPSC	Microstructured mesh-scaffolds were used to differentiate and self-organize human iPSC into trophectoderm lineage.
Miscellaneous			
[306]	Floating 3D collagen hydrogels	Organoids derived from primary murine pancreatic ductal adenocarcinoma	Organoids self-organize into highly branched and lumenized structures, replicating an in vivo-like pancreatic ductal adenocarcinoma morphology.
[307]	3D Fibrin hydrogel	Epithelial organoids	The growth of epithelial organoids was tuned by defining adhesive parameters in the used hydrogels.
[308]	Composite 3D PEG-fiber reinforced GelMa hydrogel	Keratocytes	Hydrogel constructs were used to promote regeneration of damaged corneal tissue by maintaining keratocyte identity.
[309]	3D PEG micro-wells	iPSCs, induced for cardiomyocyte differentiation	Biochemical and biophysical cues synergistically induce lineage specification, resulting in the creation of a beating human cardiac microchamber.

Table 2. Selection of representative theory work using the methods described in this review to model single cells or collectives interacting with the extracellular environment.

Study	Model	Short summary
2D single cell models		
[93]	Contour model	The tension elasticity model explains the invaginated circular arcs of contractile cells and tissues.
[95]	Contour model	The local alignment of stress fibers is included in the force balance for the cell periphery, leading to elliptical contours.
[94]	Contour model	The tension elasticity model is extended into the dynamical domain by including the flow of stress fibers.
[96]	Network model	Active contractile cable networks predict invaginated circular arcs independent of local network architecture.
[22]	Network model	Cells are modeled as a mesh of viscoelastic cables that flows in response to optogenetic activation.
[74]	Network model	Stress fibers are embedded into an active contracting network to describe energy release and changes in traction force after photoablation.
[97]	Continuum model	Analytical description of a contractile cell layer coupled to an elastic foundation.
[100]	Continuum model	Cells are described as elastic sheets and actomyosin contractility is modeled as a negative pressure.
[98]	Continuum model	Cells are modeled as elastic sheets with contractile pressure, line tension along the periphery, and adhesion depending on curvature.
[85]	Continuum model	The cell is described as a contractile sheet with viscoelastic properties adhered to an elastic substrate.
[101]	Phase field model	Motility of keratocyte fragments is described with a phase field model coupled with an orientation vector for the mean polarization of the actin network.
[107]	Cellular Potts model	Detailed model including G-protein interactions, actin fiber orientation and contraction forces to describe cell motility.
[109]	Cellular Potts model	Cell shape on micropatterns is modeled using an elastic line tension energy and linear surface tension energy.
[91]	Cellular Potts model	Cell shape and traction forces on micropatterns are modeled with a Hamiltonian using linear area and line tension and an additional elastic line tension describing stress fibers.
3D single cell models		
[121]	Network model	A mesh of active contractile cables is used to model cell shape and stress distribution in a 3D environment.
[157]	Continuum model	Three-layered model with an elastic nucleus, a viscoelastic layer representing the polymers inside the cell, and an elastic layer on the outside representing the actin cortex with mixed boundary conditions between the layers.
[161]	Continuum model	Cell nucleus and cytoplasm are modeled as hyperelastic materials, where the nucleus is five times stiffer than the cytoplasm, to predict the strain distribution in the cell.
[164]	Langevin dynamics	Cell mechanics described by Brownian Dynamics simulations of semiflexible polymers connected to extended networks.
[163]	Continuum model	The actin biochemistry of a migrating cell is explicitly modeled with a system of ordinary differential equations solved on a 3D geometry.
[159]	Continuum model	The cell is modeled with a network and a solvent field representing its cytoskeletal and cytosolic components. The evolution equation conserves mass and momentum and includes boundary conditions and constitutive relations.
[165]	Continuum model	3D cell migration and protrusion formation on a 2D substrate are modeled with a purely mechanical model describing the cell as a viscoelastic material.
[166]	Continuum model	The cell spreading process on an elastic substrate is modeled as a triple-phase system consisting of cell, substrate, and medium. The cell is modeled as an active nematic material, the medium is described as a hyperelastic material.
[160]	Continuum model	Cell indentation experiments are modeled with explicit representation of the nucleus, cytoplasm, actin, and microtubules as elastic materials.
[162]	Continuum model	Traction forces of cells in 3D are calculated from the displacement field using finite elements. Material properties of the cell and the ECM are assumed to be hyperelastic.
[156]	Phase field model	Cell migration on substrates is modeled with a 3D scalar phase field, a vector field representing mean actin fiber orientation, and additional static fields ensuring steric exclusion and actin generation only close to the surface.
[167]	Cellular Potts model	Cells are modeled as compartmentalized units consisting of the nucleus and the cytosol with elastic volume and surface constraint to describe migration through fibrous environments.
[168]	Cellular Potts model	Cells crawling on flat substrates are modeled phenomenologically by compartmentalizing the cell into cytosol, nucleus, and lamellipodia with intracellular coupling between inhibition and excitation.
[169]	Cellular Potts model	Cell migration is modeled by introducing an additional energy contribution favoring spin-copy attempts to extend the cell in regions where neighboring pixels were recently occupied by the cell.

(Continued)

Table 2. (Continued).

Study	Model	Short summary
Models for cell collectives		
[277]	Cellular Potts model	Cell sorting with two cell types is modeled by describing cells on a lattice with an elastic area constraint and interaction energies depending on neighboring cell types.
[105]	Cellular Potts model	Morphogenesis of slugs is modeled by explicitly modeling the production of cAMP and including chemotaxis to the Hamiltonian.
[106]	Cellular Potts model	Vasculogenesis is modeled by including a cell length constraint as well as chemotaxis to the Hamiltonian.
[280]	Cellular Potts model	The impact of angiogenesis on vascular tumor growth was modeled with a cellular Potts model, where the concentration of oxygen and morphogens is described with partial differential equations of the respective fields.
[278]	Cellular Potts model	Cell collectives are modeled by adding a cell–cell interface energy, cell division, and a polarity vector to model migration to describe the formation of epithelial bridges and swirls.
[279]	Cellular Potts model	Cells are described on a 2D lattice with elastic area and line tension energies. A polarization field, that is representing the cytoskeletal remodeling, describes the interaction with the substrate.
[284]	Vertex model	Cells are represented as 2D polygons, their dynamics are modeled by minimizing the total energy of the system, which consists of elastic area constraints and linear and elastic line tensions. Out-of-plane deformations of the cell sheet are observed as a result of patterned apical forces.
[317]	Vertex model	Morphogenesis of the optic cup is modeled by representing cells as polyhedrons. The system dynamics are governed by minimizing the energy, and network reconnections are possible to account for cell rearrangement, proliferation, division, and apoptosis.
[286]	Phase field model	The phase field model free energy is extended to include terms describing cell–cell and cell–substrate interactions to model cell division, adhesion, and cell sorting. Each cell is represented with a phase field.
[282]	Phase field model	Each cell is modeled as a phase field. The actin network concentration dynamics are modeled explicitly to describe cell propulsion. Cell–cell and cell–substrate interactions are modeled explicitly.
[287]	Phase field model	The phase field model is extended to describe the cell as a linearly elastic material. The forces describing the dynamics are therefore extended to include an internal elastic force and an external force density.
Models for organoids		
[316]	Vertex model	A 3D vertex model is extended to explicitly model diffusion of signaling molecules between cells. The growth and division of cells depend on the growth molecule density within the cell. The model describes epithelial expansion, evagination, and invagination.
[319]	Cellular Potts model	Lumen shape and growth are modeled with a 3D cellular Potts model with interaction energies, cell volume constraint, and a lumen area constraint. Cell division time follows a uniform distribution.
[320]	Continuum model	Crypts are modeled as cylindrical structures consisting of viscoelastic cells. Cell division, proliferation, and mechanical differences between Paneth and stem cells are modeled explicitly.
[324]	Continuum model	A reaction–diffusion model is describing the oxygen concentration in an organoid as well as in a surrounding fluid which is characterized either by continuous shaking or by laminar flow.
[321]	Continuum model	Cells in colon cancer organoids are modeled as volume fractions. Their dynamics are governed by a system of differential equations describing among others adhesion, advection, and mitosis depending on nutrient concentration.
[322]	Agent-based model	Cells are modeled as elastic objects which differentiate due to Wnt- and Notch-signaling. The cells interact with a semi-flexible, elastic polymer network representing the extracellular environment to model organoid formation.

complemented by standardization through cell lines, which usually are transformed cells that can proliferate without limits. Despite these advances in quantification and standardization, it remained challenging to cultivate distinct cellular populations in the absence of their natural growth environment.

Three decades ago, this situation changed dramatically with the advent of mechanobiology, which demonstrated that physical aspects of the extracellular environment (in particular stiffness, geometry, and topography) play an equally important role for cellular decision making as do biochemical factors. Maybe the most decisive factor for this development was the transfer of new methods from materials science into cell biology and biophysics: starting with PDMS-technology, microcontact printing, and photolithography, it has become customary to prepare mechanically and geometrically defined environments for cell culture. Biol-

ogists teamed up with physicists, chemists, material scientists, and engineers in order to develop sophisticated cell culture platforms by microfabrication, for example by direct laser writing of cell culture scaffolds in three dimensions. These experimental developments were complemented by advances in quantitative image processing and modeling. First applied to single cells, these tools are now increasingly applied to cell collectives, from cell monolayers to 3D spheroids and organoids.

Thanks to these interdisciplinary approaches, we are nowadays in the exciting position to take the next step. As the field has grown from single cells toward multicellular systems, it should be the scope of future research to merge the knowledge from biochemistry, molecular biology, and biophysics to control cellular growth and behavior in vitro. The emergence of the organoid technology is a prime example in this regard. As described in the

Table 3. Overview of established model frameworks to describe single cells or cell collectives with their advantages and limitations.

Model	Mechanism	Application areas	Advantages	Limitations
Contour model	Force balance between line and surface tensions	Cell shape in structured environments	Simple, fast, straightforward	Only describes static cell shapes in 2D
Network model	Cells are described with cables and springs representing the cytoskeleton	Cell shape and force distribution, optogenetic, and laser cutting experiments can be modeled	Explicit network description of the cytoskeleton	Dynamics, migration, and cell-cell interactions are difficult to include
Continuum model	Single cells or collectives are described as active visco-elastic materials	Cell shape and force distribution	Parameters such as stiffness and viscosity can be obtained from experiment	Cells are usually modeled as isotropic materials
Cellular Potts model	Energy-based description on a lattice	Single or collective cell shape and migration, tissue morphology	Dynamic description, appropriate framework to model complex systems	Difficult to describe forces, parameters do not correspond to measurable quantities
Phase field model	Energy-based description of the cell boundary	Single or collective cell migration	Dynamic description of the cell boundary in 3D in complex environments	Internal structure of the cell is represented with a polarization vector
Vertex model	Force-based description of cell collectives, cells are represented as polyeders	Cell monolayers, tissue morphology	Can bridge the gap between local force generation and tissue deformation	Only suitable for tightly packed collectives such as epithelial tissue

section above, fate induction in organoids is first established biochemically, while scaffolds with tuned elasticity and microtopography later help to guide the growing spheroids into structured tissues with a function. Future studies in this direction are expected and bear the potential to take another step toward organs-in-a-dish. One interesting direction is the transition from 2D to 3D culture systems. More refined methods in microfabrication and molecular biology allow us to tackle the recreation of multilayered and stratified tissues in 3D, for example of an artificial retina. Mathematical models might help to accelerate this process and to suggest interesting designs, thus avoiding delays or dead ends in experimentation. The contribution of materials science does not need to be confined to spatial and mechanical aspects, but also could cover the time domain. Stimuli-responsive

materials and optogenetics can be used to implement temporal protocols to guide cell development or even to implement feedback loops that automatically adjust the physical properties of the environment to the current state of the biological system. Bringing together these different technologies opens up numerous exciting and very promising new avenues for the control of cells, tissues, and organs.

Acknowledgements

R.L. and K.W. contributed equally to this work. All authors acknowledge support by the cluster of excellence 3DMM2O (EXC 2082/1-390761711) funded by the Deutsche Forschungsgemeinschaft (DFG, German Research Foundation) under Germany's Excellence Strategy.

Open access funding enabled and organized by Projekt DEAL.

Conflict of Interest

The authors declare no conflict of interest.

Keywords

adhesive micropatterning, cell culture scaffolds, cell mechanics, direct laser writing, microfabrication, tissues, cell adhesion

Received: February 23, 2023

Revised: April 11, 2023

Published online:

- [1] T. Iskratsch, H. Wolfenson, M. P. Sheetz, *Nat. Rev. Mol. Cell Biol.* **2014**, *15*, 825.
- [2] V. Ruprecht, P. Monzo, A. Rvasio, Z. Yue, E. Makhija, P. O. Strale, N. Gauthier, G. v. Shivashankar, V. Studer, C. Albiges-Rizo, V. Viasnoff, *J. Cell Sci.* **2017**, *130*, 51.
- [3] C. S. Chen, M. Mrksich, S. Huang, G. M. Whitesides, D. E. Ingber, *Science* **1997**, *276*, 1425.
- [4] S. Dupont, L. Morsut, M. Aragona, E. Enzo, S. Giulitti, M. Cordenonsi, F. Zanconato, J. le Digabel, M. Forcato, S. Bicciato, N. Elvassore, S. Piccolo, *Nature* **2011**, *474*, 179.
- [5] T. Oliver, K. Jacobson, M. Dembo, *Cell Motil. Cytoskeleton* **1995**, *31*, 225.
- [6] M. Dembo, Y. L. Wang, *Biophys. J.* **1999**, *76*, 2307.
- [7] R. J. Pelham, Y. L. Wang, *Proc. Natl. Acad. Sci. USA* **1997**, *94*, 13661.
- [8] A. J. Engler, S. Sen, H. L. Sweeney, D. E. Discher, *Cell* **2006**, *126*, 677.
- [9] R. McBeath, D. M. Pirone, C. M. Nelson, K. Bhadriraju, C. S. Chen, *Dev. Cell* **2004**, *6*, 483.
- [10] I. Andreu, I. Granero-Moya, N. R. Chahare, K. Clein, M. Molina-Jordán, A. E. M. Beedle, A. Elosegui-Artola, J. F. Abenza, L. Rossetti, X. Trepát, B. Raveh, P. Roca-Cusachs, *Nat. Cell Biol.* **2022**, *24*, 896.
- [11] R. Sunyer, V. Conte, J. Escribano, A. Elosegui-Artola, A. Labernadie, L. Valon, D. Navajas, J. M. García-Aznar, J. J. Muñoz, P. Roca-Cusachs, X. Trepát, *Science* **2016**, *353*, 1157.
- [12] E. Garreta, R. D. Kamm, S. M. Chuva de Sousa Lopes, M. A. Lancaster, R. Weiss, X. Trepát, I. Hyun, N. Montserrat, *Nat. Mater.* **2020**, *20*, 145.
- [13] M. Hofer, M. P. Lutolf, *Nat. Rev. Mater.* **2021**, *6*, 402.
- [14] M. R. Blatchley, K. S. Anseth, *Nat. Rev. Bioeng.* **2023**, *1*, 329.
- [15] S. van Helvert, C. Storm, P. Friedl, *Nat. Cell Biol.* **2018**, *20*, 8.
- [16] J. Laurent, G. Blin, F. Chatelain, V. Vanneaux, A. Fuchs, J. Larghero, M. Théry, *Nat. Biomed. Eng.* **2017**, *1*, 939.
- [17] J. Huisken, J. Swoger, F. del Bene, J. Wittbrodt, E. H. K. Stelzer, *Science* **2004**, *305*, 1007.
- [18] F. Pampaloni, E. G. Reynaud, E. H. K. Stelzer, *Nat. Rev. Mol. Cell Biol.* **2007**, *8*, 839.
- [19] D. Li, L. Shao, B. C. Chen, X. Zhang, M. Zhang, B. Moses, D. E. Millie, J. R. Beach, J. A. Hammer, M. Pasham, T. Kirchhausen, M. A. Baird, M. W. Davidson, P. Xu, E. Betzig, *Science* **2015**, *349*.
- [20] O. Campàs, T. Mammoto, S. Hasso, R. A. Sperling, D. O'Connell, A. G. Bischof, R. Maas, D. A. Weitz, L. Mahadevan, D. E. Ingber, *Nat. Methods* **2013**, *11*, 183.
- [21] P. H. Wu, D. R. ben Aroush, A. Asnacios, W. C. Chen, M. E. Dokukin, B. L. Doss, P. Durand-Smet, A. Ekpenyong, J. Guck, N. v. Guz, P. A. Janmey, J. S. H. Lee, N. M. Moore, A. Ott, Y. C. Poh, R. Ros, M. Sander, I. Sokolov, J. R. Staunton, N. Wang, G. Whyte, D. Wirtz, *Nat. Methods* **2018**, *15*, 491.
- [22] P. W. Oakes, E. Wagner, C. A. Brand, D. Probst, M. Linke, U. S. Schwarz, M. Glotzer, M. L. Gardel, *Nat. Commun.* **2017**, *8*, 15817.
- [23] F. Klein, B. Richter, T. Striebel, C. M. Franz, G. von Freymann, M. Wegener, M. Bastmeyer, *Adv. Mater.* **2011**, *23*, 1341.
- [24] M. Hippler, E. D. Lemma, S. Bertels, E. Blasco, C. Barner-Kowollik, M. Wegener, M. Bastmeyer, *Adv. Mater.* **2019**, *31*, 1808110.
- [25] E. Karzbrun, A. H. Khankhel, H. C. Megale, S. M. K. K. Glasauer, Y. Wyle, G. Britton, A. Warmflash, K. S. Kosik, E. D. Siggia, B. I. Shraiman, S. J. Streichan, *Nature* **2021**, *599*, 268.
- [26] N. Gjorevski, M. Nikolaev, T. E. Brown, O. Mitrofanova, N. Brandenberg, F. W. DelRio, F. M. Yavitt, P. Liberali, K. S. Anseth, M. P. Lutolf, *Science* **2022**, *375*, eaaw9021.
- [27] P. J. Albert, U. S. Schwarz, *Cell Adh. Migr.* **2016**, *10*, 516.
- [28] B. Alberts (Ed.), *Molecular Biology of the Cell*, 6th ed., Garland Science, New York, NY **2015**.
- [29] C. Lorenz, S. Köster, *Biophys. Rev.* **2022**, *3*, 031304.
- [30] P. Niethammer, *Annu. Rev. Cell Dev. Biol.* **2021**, *37*, 233.
- [31] U. S. Schwarz, *Soft Matter* **2007**, *3*, 263.
- [32] A. J. Lomakin, C. J. Cattin, D. Cuvelier, Z. Alraies, M. Molina, G. P. F. Nader, N. Srivastava, P. J. Saez, J. M. Garcia-Arcos, I. Y. Zhitnyak, A. Bhargava, M. K. Driscoll, E. S. Welf, R. Fiolka, R. J. Petrie, N. S. de Silva, J. M. González-Granado, N. Manel, A. M. Lennon-Dumenil, D. J. Müller, M. Piel, *Science* **2020**, *370*, 2894.
- [33] J. Renkawitz, A. Kopf, J. Stopp, I. de Vries, M. K. Driscoll, J. Merrin, R. Hauschild, E. S. Welf, G. Danuser, R. Fiolka, M. Sixt, *Nature* **2019**, *568*, 546.
- [34] B. Geiger, J. P. Spatz, A. D. Bershadsky, *Nat. Rev. Mol. Cell Biol.* **2009**, *10*, 21.
- [35] J. D. Humphries, M. R. Chastney, J. A. Askari, M. J. Humphries, *Curr. Opin. Cell Biol.* **2019**, *56*, 14.
- [36] D. E. Discher, P. Janmey, Y. L. Wang, *Science* **2005**, *310*, 1139.
- [37] A. Isomursu, K. Y. Park, J. Hou, B. Cheng, M. Mathieu, G. A. Shamsan, B. Fuller, J. Kasim, M. M. Mahmoodi, T. J. Lu, G. M. Genin, F. Xu, M. Lin, M. D. Distefano, J. Ivaska, D. J. Odde, *Nat. Mater.* **2022**, *21*, 1081.
- [38] M. Théry, *J. Cell Sci.* **2010**, *123*, 4201.
- [39] S. J. P. P. Callens, R. J. C. C. Uyttendaele, L. E. Fratila-Apachitei, A. A. Zadpoor, *Biomaterials* **2020**, *232*, 119739.
- [40] B. Ladoux, R. M. Mège, X. Trepát, *Trends Cell Biol.* **2016**, *26*, 420.
- [41] M. Raab, J. Swift, P. C. D. P. Dingal, P. Shah, J. W. Shin, D. E. Discher, *J. Cell Biol.* **2012**, *199*, 669.
- [42] A. Zemel, F. Rehfeldt, A. E. X. Brown, D. E. Discher, S. A. Safran, *Nat. Phys.* **2010**, *6*, 468.
- [43] M. Théry, A. Pépin, E. Dressaire, Y. Chen, M. Bornens, *Cell Motil. Cytoskeleton* **2006**, *63*, 341.
- [44] J. P. Califano, C. A. Reinhart-King, *Cell Mol. Bioeng.* **2010**, *3*, 68.
- [45] C. M. Lo, H. B. Wang, M. Dembo, Y. L. Wang, *Biophys. J.* **2000**, *79*, 144.
- [46] C. A. Deforest, K. S. Anseth, *Annu. Rev. Chem. Biomol. Eng.* **2012**, *3*, 421.
- [47] D. Missirlis, J. P. Spatz, *Biomacromolecules* **2014**, *15*, 195.
- [48] W. Wang, Y.-B. Li, C. L. Lay, H. Q. Liu, H. R. Tan, K. Engberg, C. W. Frank, *Biomed. Mater.* **2011**, *6*, 055006.
- [49] G. Huang, L. Wang, S. Wang, Y. Han, J. Wu, Q. Zhang, F. Xu, T. J. Lu, *Biofabrication* **2012**, *4*, 042001.
- [50] M. Guvendiren, J. A. Burdick, *Curr. Opin. Biotechnol.* **2013**, *24*, 841.
- [51] D. Li, H. Colin-York, L. Barbieri, Y. Javanmardi, Y. Guo, K. Korobchevskaya, E. Moeendarbary, D. Li, M. Fritzsche, *Nat. Commun.* **2021**, *12*, 1.
- [52] N. Q. Balaban, U. S. Schwarz, D. Riveline, P. Goichberg, G. Tzur, I. Sabanay, D. Mahalu, S. Safran, A. Bershadsky, L. Addadi, B. Geiger, *Nat. Cell Biol.* **2001**, *3*, 466.
- [53] P. Moshayedi, L. Da F Costa, A. Christ, S. P. Lacour, J. Fawcett, J. Guck, K. Franze, *J. Phys.: Condens. Matter* **2010**, *22*, 194114.
- [54] E. E. Charrier, K. Pogoda, R. Li, C. Y. Park, J. J. Fredberg, P. A. Janmey, *APL Bioeng.* **2020**, *4*, 036104.

- [55] E. Gutierrez, E. Tkachenko, A. Besser, P. Sundd, K. Ley, G. Danuser, M. H. Ginsberg, A. Groisman, *PLoS One* **2011**, *6*, e23807.
- [56] V. Heinrichs, S. Dieluweit, J. Stellbrink, W. Pyckhout-Hintzen, N. Hersch, D. Richter, R. Merkel, *PLoS One* **2018**, *13*, e0195180.
- [57] C. M. Nelson, R. P. Jean, J. L. Tan, W. F. Liu, N. J. Sniadecki, A. A. Spector, C. S. Chen, *Proc. Natl. Acad. Sci. U. S. A.* **2005**, *102*, 11594.
- [58] J. H. Wen, L. G. Vincent, A. Fuhrmann, Y. S. Choi, K. C. Hribar, H. Taylor-Weiner, S. Chen, A. J. Engler, *Nat. Mater.* **2014**, *13*, 979.
- [59] D. Falconnet, G. Csucs, H. M. Grandin, M. Textor, *Biomaterials* **2006**, *27*, 3044.
- [60] M. Mrksich, C. S. Chen, Y. Xia, L. E. Dike, D. E. Ingber, G. M. Whitesides, *Proc. Natl. Acad. Sci. U. S. A.* **1996**, *93*, 10775.
- [61] N. C. Gauthier, M. A. Fardin, P. Roca-Cusachs, M. P. Sheetz, *Proc. Natl. Acad. Sci. U. S. A.* **2011**, *108*, 14467.
- [62] P. Hotulainen, P. Lappalainen, *J. Cell Biol.* **2006**, *173*, 383.
- [63] E. Kassianidou, D. Probst, J. Jäger, S. Lee, A. L. Roguet, U. S. Schwarz, S. Kumar, *Cell Rep.* **2019**, *27*, 1897.
- [64] S. Jalal, S. Shi, V. Acharya, R. Y. J. Huang, V. Viasnoff, A. D. Bershadsky, Y. H. Tee, *J. Cell Sci.* **2019**, *132*, 5.
- [65] Y. H. Tee, T. Shemesh, V. Thiagarajan, R. F. Hariadi, K. L. Anderson, C. Page, N. Volkmann, D. Hanein, S. Sivaramakrishnan, M. M. Kozlov, A. D. Bershadsky, *Nat. Cell Biol.* **2015**, *17*, 445.
- [66] P. Maiuri, E. Terriac, P. Paul-Gilloteaux, T. Vignaud, K. McNally, J. Onuffer, K. Thorn, P. A. Nguyen, N. Georgoulia, D. Soong, A. Jayo, N. Beil, J. Beneke, J. C. Hong Lim, C. Pei-Ying Sim, Y. S. Chu, A. Jiménez-Dalmaroni, J. F. Joanny, J. P. Thiery, H. Erfle, M. Parsons, T. J. Mitchison, W. A. Lim, A. M. Lennon-Duménil, M. Piel, M. Théry, *Curr. Biol.* **2012**, *22*, R673.
- [67] D. B. Brückner, A. Fink, C. Schreiber, P. J. F. Röttgermann, J. O. Rädler, C. P. Broedersz, *Nat. Phys.* **2019**, *15*, 595.
- [68] J. L. Tan, J. Tien, D. M. Pirone, D. S. Gray, K. Bhadriraju, C. S. Chen, *Proc. Natl. Acad. Sci. U. S. A.* **2003**, *100*, 1484.
- [69] P. Maiuri, J. F. Rupprecht, S. Wieser, V. Rupprecht, O. Bénichou, N. Carpi, M. Coppey, S. De Beco, N. Gov, C. P. Heisenberg, C. Lage Crespo, F. Lautenschlaeger, M. Le Berre, A. M. Lennon-Duménil, M. Raab, H. R. Thiam, M. Piel, M. Sixt, R. Voituriez, *Cell* **2015**, *161*, 374.
- [70] T. J. Autenrieth, S. C. Frank, A. M. Greiner, D. Klumpp, B. Richter, M. Hauser, S. Il Lee, J. Levine, M. Bastmeyer, *Integr. Biol.* **2016**, *8*, 1067.
- [71] A. D. Rape, W. H. Guo, Y. L. Wang, *Biomaterials* **2011**, *32*, 2043.
- [72] Q. Tseng, I. Wang, E. Duchemin-Pelletier, A. Azoune, N. Carpi, J. Gao, O. Filhol, M. Piel, M. Théry, M. Balland, *Lab Chip* **2011**, *11*, 2231.
- [73] U. S. Schwarz, J. R. D. Soiné, *Biochim. Biophys. Acta, Mol. Cell Res.* **2015**, *1853*, 3095.
- [74] T. Vignaud, C. Copos, C. Leterrier, M. Toro-Nahuelpan, Q. Tseng, J. Mahamid, L. Blanchoin, A. Mogilner, M. Théry, L. Kurzawa, *Nat. Mater.* **2020**, *20*, 410.
- [75] M. Gupta, L. Kocgozlu, B. R. Sarangi, F. Margadant, M. Ashraf, B. Ladoux, *Methods Cell Biol.* **2015**, *125*, 289.
- [76] A. Ganz, M. Lambert, A. Saez, P. Silberzan, A. Buguin, R. Ren´, R. Marc, B. B. Ladoux, *Biol. Cell.* **2006**, *98*, 721.
- [77] I. Schoen, W. Hu, E. Klotzsch, V. Vogel, *Nano Lett.* **2010**, *10*, 1823.
- [78] J. H. Hughes, S. Kumar, *Curr. Opin. Biotechnol.* **2016**, *40*, 82.
- [79] T. Wittmann, A. Dema, J. van Haren, *Curr. Opin. Cell Biol.* **2020**, *66*, 1.
- [80] Y. I. Wu, D. Frey, O. I. Lungu, A. Jaehrig, I. Schlichting, B. Kuhlman, K. M. Hahn, *Nature* **2009**, *461*, 104.
- [81] S. de Beco, K. Vaidziulytė, J. Manzi, F. Dalier, F. di Federico, G. Cornilleau, M. Dahan, M. Coppey, *Nat. Commun.* **2018**, *9*, 4816.
- [82] K. Hennig, I. Wang, P. Moreau, L. Valon, S. DeBeco, M. Coppey, Y. A. Miroshnikova, C. Albiges-Rizo, C. Favard, R. Voituriez, M. Balland, *Sci. Adv.* **2020**, *6*, 5670.
- [83] A. Hadjitheodorou, G. R. R. Bell, F. Ellett, S. Shastry, D. Irimia, S. R. Collins, J. A. Theriot, *Nat. Commun.* **2021**, *12*, 6619.
- [84] L. Valon, A. Marin-Llauradó, T. Wyatt, G. Charras, X. Trepat, *Nat. Commun.* **2017**, *8*, 14396.
- [85] T. Andersen, D. Wörthmüller, D. Probst, I. Wang, P. Moreau, V. Fitzpatrick, T. Boudou, U. S. Schwarz, M. Balland, *Biophys. J.* **2023**, *112*, 684.
- [86] G. A. Dunn, J. P. Heath, *Exp. Cell Res.* **1976**, *101*, 1.
- [87] L. Pieuchot, J. Marteau, A. Guignandon, T. Dos Santos, I. Brigaud, P. F. Chauvy, T. Cloatre, A. Ponche, T. Petithory, P. Rougerie, M. Vassaux, J. L. Milan, N. Tusamda Wakhloo, A. Spangenberg, M. Bigerelle, K. Anselme, *Nat. Commun.* **2018**, *9*, 3995.
- [88] M. Werner, S. B. G. Blanquer, S. P. Haimi, G. Korus, J. W. C. Dunlop, G. N. Duda, D. W. Grijpma, A. Petersen, *Adv. Sci.* **2017**, *4*, 1600347.
- [89] U. S. Schwarz, S. A. Safran, *Rev. Mod. Phys.* **2013**, *85*, 1327.
- [90] P. Kollmannsberger, C. M. Bidan, J. W. C. Dunlop, P. Fratzl, *Soft Matter* **2011**, *7*, 9549.
- [91] P. J. Albert, U. S. Schwarz, *Biophys. J.* **2014**, *106*, 2340.
- [92] I. B. Bischofs, S. S. Schmidt, U. S. Schwarz, *Phys. Rev. Lett.* **2009**, *103*, 048101.
- [93] I. B. Bischofs, F. Klein, D. Lehnert, M. Bastmeyer, U. S. Schwarz, *Biophys. J.* **2008**, *95*, 3488.
- [94] K. Weißenbruch, J. Grewe, M. Hippler, M. Fladung, M. Tremmel, K. Stricker, U. S. Schwarz, M. Bastmeyer, *Elife* **2021**, *10*, 71888.
- [95] K. Schakenraad, J. Ernst, W. Pomp, E. H. J. Danen, R. M. H. Merks, T. Schmidt, L. Giomi, *Soft Matter* **2020**, *16*, 6328.
- [96] P. Guthardt Torres, I. B. Bischofs, U. S. Schwarz, *Phys. Rev. E: Stat., Nonlinear, Soft Matter Phys.* **2012**, *85*, 011913.
- [97] C. M. Edwards, U. S. Schwarz, *Phys. Rev. Lett.* **2011**, *107*, 128101.
- [98] P. W. Oakes, S. Banerjee, M. C. Marchetti, M. L. Gardel, *Biophys. J.* **2014**, *107*, 825.
- [99] J. Prost, F. Jülicher, J. F. Joanny, *Nat. Phys.* **2015**, *11*, 111.
- [100] R. Bikwemu, A. J. Wolfe, X. Xing, J. J. Zhang, Z. Liu, B. B. Guo, S. Banerjee, M. C. Marchetti, *New J. Phys.* **2013**, *15*, 35015.
- [101] F. Ziebert, S. Swaminathan, I. S. Aranson, *J. R. Soc. Interface* **2012**, *9*, 1084.
- [102] A. Karma, D. A. Kessler, H. Levine, *Phys. Rev. Lett.* **2001**, *87*, 045501.
- [103] A. Moure, H. Gomez, *Arch. Comput. Methods Eng.* **2021**, *28*, 311.
- [104] F. Graner, J. A. Glazier, *Phys. Rev. Lett.* **1992**, *69*, 2013.
- [105] N. Savill, P. Hogeweg, *J. Theor. Biol.* **1997**, *197*, 229.
- [106] R. M. H. Merks, S. v. Brodsky, M. S. Gligorksy, S. A. Newman, J. A. Glazier, *Dev. Biol.* **2006**, *289*, 44.
- [107] A. F. M. Marée, A. Jilkine, A. Dawes, V. A. Grieneisen, L. Edelstein-Keshet, *Bull. Math. Biol.* **2006**, *68*, 1169.
- [108] A. F. M. Marée, V. A. Grieneisen, P. Hogeweg, *Single Cell based Models in Biology and Medicine* (Eds: A. R. A. Anderson, M. A. J. Chaplain, K. A. Rejniak), Birkhäuser, Basel **2007**.
- [109] B. Vianay, J. Käfer, E. Planus, M. Block, F. Graner, H. Guillou, *Phys. Rev. Lett.* **2010**, *105*, 128101.
- [110] E. Cukierman, R. Pankov, D. R. Stevens, K. M. Yamada, *Science* **2001**, *294*, 1708.
- [111] B. M. Baker, C. S. Chen, *J. Cell Sci.* **2012**, *125*, 3015.
- [112] C. S. Chen, *Trends Cell Biol.* **2016**, *26*, 798.
- [113] J. L. Young, A. W. Holle, J. P. Spatz, *Exp. Cell Res.* **2016**, *343*, 3.
- [114] F. Grinnell, *Trends Cell Biol.* **2003**, *13*, 264.
- [115] K. M. Yamada, M. Sixt, *Nat. Rev. Mol. Cell Biol.* **2019**, *20*, 738.
- [116] J. S. Harunaga, K. M. Yamada, *Matrix Biol.* **2011**, *30*, 363.
- [117] M. L. Kutys, C. S. Chen, *Curr. Opin. Cell Biol.* **2016**, *42*, 73.
- [118] G. Huang, F. Li, X. Zhao, Y. Ma, Y. Li, M. Lin, G. Jin, T. J. Lu, G. M. Genin, F. Xu, *Chem. Rev.* **2017**, *117*, 12764.
- [119] G. Velve-Casquillas, M. Le Berre, M. Piel, P. T. Tran, *Nano Today* **2010**, *5*, 28.
- [120] F. J. Vernerey, S. Lalitha Sridhar, A. Muralidharan, S. J. Bryant, *Chem. Rev.* **2021**, *121*, 11085.

- [121] C. A. Brand, M. Linke, K. Weissenbruch, B. Richter, M. Bastmeyer, U. S. Schwarz, *Biophys. J.* **2017**, *113*, 770.
- [122] M. S. Hall, R. Long, X. Feng, Y. L. Huang, C. Y. Hui, M. Wu, *Exp. Cell Res.* **2013**, *319*, 2396.
- [123] R. S. Stowers, S. C. Allen, L. J. Suggs, K. S. Anseth, *Proc. Natl. Acad. Sci. U. S. A.* **2015**, *112*, 1953.
- [124] J. M. Lee, W. Y. Yeong, *Adv. Healthcare Mater.* **2016**, *5*, 2856.
- [125] K. Pataky, T. Braschler, A. Negro, P. Renaud, M. P. Lutolf, J. Brugger, *Adv. Mater.* **2012**, *24*, 391.
- [126] E. D. Tabdanov, V. Puram, A. Zhovmer, P. P. Provenzano, *Cell Rep.* **2018**, *25*, 328.
- [127] E. D. Tabdanov, N. J. Rodríguez-Merced, A. X. Cartagena-Rivera, V. V. Puram, M. K. Callaway, E. A. Ensminger, A. J. Pomeroy, K. Yamamoto, W. S. Lahr, B. R. Webber, B. S. Moriarity, A. S. Zhovmer, P. P. Provenzano, *Nat. Commun.* **2021**, *12*, 2815.
- [128] N. Minc, D. Burgess, F. Chang, *Cell* **2011**, *144*, 414.
- [129] K. Sheets, J. Wang, W. Zhao, R. Kapania, A. S. Nain, *Biophys. J.* **2016**, *111*, 197.
- [130] M. Bao, J. Xie, A. Piruska, W. T. S. Huck, *Nat. Commun.* **2017**, *8*, 1.
- [131] Y. Sharma, A. Tiwari, S. Hattori, D. Terada, A. K. Sharma, M. Ramalingam, H. Kobayashi, *Int. J. Biol. Macromol.* **2012**, *51*, 627.
- [132] T. Scheibel, *Microb. Cell Fact.* **2004**, *3*, 14.
- [133] A. Lazaris, S. Arcidiacono, Y. Huang, J. F. Zhou, F. Duguay, N. Chretien, E. A. Welsh, J. W. Soares, C. N. Karatzas, *Science* **2002**, *295*, 472.
- [134] J. A. Matthews, G. E. Wnek, D. G. Simpson, G. L. Bowlin, *Biomacromolecules* **2002**, *3*, 232.
- [135] K. S. Rho, L. Jeong, G. Lee, B. M. Seo, Y. J. Park, S. D. Hong, S. Roh, J. J. Cho, W. H. Park, B. M. Min, *Biomaterials* **2006**, *27*, 1452.
- [136] Z. M. Huang, Y. Z. Zhang, S. Ramakrishna, C. T. Lim, *Polymer* **2004**, *45*, 5361.
- [137] M. Li, M. J. Mondrinos, M. R. Gandhi, F. K. Ko, A. S. Weiss, P. I. Lelkes, *Biomaterials* **2005**, *26*, 5999.
- [138] J. Nam, J. Johnson, J. J. Lannutti, S. Agarwal, *Acta Biomater.* **2011**, *7*, 1516.
- [139] L. Yu, J. Li, J. Hong, Y. Takashima, N. Fujimoto, M. Nakajima, A. Yamamoto, X. Dong, Y. Dang, Y. Hou, W. Yang, I. Minami, K. Okita, M. Tanaka, C. Luo, F. Tang, Y. Chen, C. Tang, H. Kotera, L. Liu, *Stem Cell Rep.* **2018**, *11*, 142.
- [140] Z. Ma, M. Kotaki, R. Inai, S. Ramakrishna, *Tissue Eng.* **2005**, *11*, 101.
- [141] S. Kidoaki, I. K. Kwon, T. Matsuda, *Biomaterials* **2005**, *26*, 37.
- [142] A. M. Smith, E. F. Banwell, W. R. Edwards, M. J. Pandya, D. N. Woolfson, *Adv. Funct. Mater.* **2006**, *16*, 1022.
- [143] T. Bentele, F. Amadei, E. Kimmle, M. Veschgini, P. Linke, M. Sontag-González, J. Tennigkeit, A. D. Ho, S. Özbek, M. Tanaka, *Sci. Rep.* **2019**, *9*, 19116.
- [144] K. Hayashi, M. Matsuda, M. Nakahata, Y. Takashima, M. Tanaka, *Polymers* **2022**, *14*, 4407.
- [145] S. Bongiovanni Abel, F. Montini Ballarin, G. A. Abraham, *Nanotechnology* **2020**, *31*, 172002.
- [146] W. Pattanapiboon, P. Nakmahachalasint, *Electron. Lett.* **2021**, *57*, 799.
- [147] A. S. Nain, J. A. Phillippi, M. Sitti, J. MacKrell, P. G. Campbell, C. Amon, *Small* **2008**, *4*, 1153.
- [148] A. Jana, I. Nookaew, J. Singh, B. Behkam, A. T. Franco, A. S. Nain, *FASEB J.* **2019**, *33*, 10618.
- [149] D. Huang, Y. Nakamura, A. Ogata, S. Kidoaki, *Polym. J.* **2020**, *52*, 333.
- [150] A. M. Greiner, B. Richter, M. Bastmeyer, *Macromol. Biosci.* **2012**, *12*, 1301.
- [151] F. Klein, T. Striebel, J. Fischer, Z. Jiang, C. M. Franz, G. Von Freymann, M. Wegener, M. Bastmeyer, *Adv. Mater.* **2010**, *22*, 868.
- [152] A. M. Greiner, F. Klein, T. Gudzenko, B. Richter, T. Striebel, B. G. Wundari, T. J. Autenrieth, M. Wegener, C. M. Franz, M. Bastmeyer, *Biomaterials* **2015**, *69*, 121.
- [153] N. Silbernagel, A. Körner, J. Balitzki, M. Jaggy, S. Bertels, B. Richter, M. Hippler, A. Hellwig, M. Hecker, M. Bastmeyer, N. D. Ullrich, *Biomaterials* **2020**, *227*, 119551.
- [154] S. Bertels, M. Jaggy, B. Richter, S. Keppler, K. Weber, E. Genthner, A. C. Fischer, M. Thiel, M. Wegener, A. M. Greiner, T. J. Autenrieth, M. Bastmeyer, *Sci. Rep.* **2021**, *11*, 9269.
- [155] M. Hippler, K. Weissenbruch, K. Richler, E. D. Lemma, M. Nakahata, B. Richter, C. Barner-Kowollik, Y. Takashima, A. Harada, E. Blasco, M. Wegener, M. Tanaka, M. Bastmeyer, *Sci. Adv.* **2020**, *6*, 2648.
- [156] B. Winkler, I. S. Aranson, F. Ziebert, *Commun. Phys.* **2019**, *2*, 82.
- [157] R. Ananthakrishnan, J. Guck, F. Wottawah, S. Schinkinger, B. Lincoln, M. Romeyke, T. Moon, J. Käs, *J. Theor. Biol.* **2006**, *242*, 502.
- [158] M. Herant, M. Dembo, *J. Comput. Biol.* **2010**, *17*, 1639.
- [159] M. Herant, M. Dembo, *Biophys. J.* **2010**, *98*, 1408.
- [160] W. Yang, D. Lacroix, L. P. Tan, J. Chen, *J. Mater. Res.* **2021**, *36*, 2591.
- [161] E. Gladilin, A. Micoulet, B. Hosseini, K. Rohr, J. Spatz, R. Eils, *Phys. Biol.* **2007**, *4*, 104.
- [162] S. Hervas-Raluy, M. J. Gomez-Benito, C. Borau-Zamora, M. Córdor, J. M. Garcia-Aznar, *PLoS One* **2021**, *16*, e0249018.
- [163] J. A. Ditlev, N. M. Vacanti, I. L. Novak, L. M. Loew, *Biophys. J.* **2009**, *96*, 3529.
- [164] F. Nedelec, D. Foethke, *New J. Phys.* **2007**, *9*, 427.
- [165] R. Allena, *Bull. Math. Biol.* **2013**, *75*, 288.
- [166] H. Fan, S. Li, *Biomech. Model. Mechanobiol* **2015**, *14*, 1265.
- [167] M. Scianna, L. Preziosi, K. Wolf, *Math. Biosci. Eng.* **2013**, *10*, 235.
- [168] I. Fortuna, G. C. Perrone, M. S. Krug, E. Susin, J. M. Belmonte, G. L. Thomas, J. A. Glazier, R. M. C. de Almeida, *Biophys. J.* **2020**, *118*, 2801.
- [169] I. M. N. Wortel, I. Niculescu, P. M. Kolijn, N. S. Gov, R. J. de Boer, J. Textor, *Biophys. J.* **2021**, *120*, 2609.
- [170] W. R. Holmes, L. Edelstein-Keshet, *PLoS Comput. Biol.* **2012**, *8*, e1002793.
- [171] P. J. Albert, U. S. Schwarz, *Integr. Biol.* **2016**, *8*, 741.
- [172] M. Zinner, I. Lukonin, P. Liberali, *Curr. Opin. Cell Biol.* **2020**, *67*, 37.
- [173] C. Frantz, K. M. Stewart, V. M. Weaver, *J. Cell Sci.* **2010**, *123*, 4195.
- [174] Q. Wen, P. A. Janmey, *Exp. Cell Res.* **2013**, *319*, 2481.
- [175] M. A. Garcia, W. J. Nelson, N. Chavez, *Cold Spring Harbor Perspect. Biol.* **2018**, *10*, a029181.
- [176] M. Bachmann, S. Kukkurainen, V. P. Hytonen, B. Wehrle-Haller, *Physiol. Rev.* **2019**, *99*, 1655.
- [177] G. Charras, A. S. Yap, *Curr. Biol.* **2018**, *28*, R445.
- [178] J. T. Parsons, A. R. Horwitz, M. A. Schwartz, *Nat. Rev. Mol. Cell Biol.* **2010**, *11*, 633.
- [179] O. Chaudhuri, J. Cooper-White, P. A. Janmey, D. J. Mooney, V. B. Shenoy, *Nature* **2020**, *584*, 535.
- [180] N. Bonakdar, R. Gerum, M. Kuhn, M. Sporrer, A. Lippert, W. Schneider, K. E. Aifantis, B. Fabry, *Nat. Mater.* **2016**, *15*, 1090.
- [181] A. J. Hughes, H. Miyazaki, M. C. Coyle, J. Zhang, M. T. Laurie, D. Chu, Z. Vavrusova, R. A. Schneider, O. D. Klein, Z. J. Gartner, *Dev. Cell* **2018**, *44*, 165.
- [182] M. Tozluoglu, M. Duda, N. J. Kirkland, R. Barrientos, J. J. Burden, J. J. Munoz, Y. Mao, *Dev. Cell* **2019**, *51*, 299.
- [183] A. E. Shyer, T. Tallinen, N. L. Nerurkar, Z. Wei, E. S. Gil, D. L. Kaplan, C. J. Tabin, L. Mahadevan, *Science* **2013**, *342*, 212.
- [184] S. J. P. Callens, R. J. C. Uyttendaele, L. E. Fratila-Apachitei, A. A. Zadpoor, *Biomaterials* **2020**, *232*, 119739.
- [185] C. M. Nelson, *J. Biomech. Eng.* **2016**, *138*, 21005.
- [186] H. G. Yevick, P. W. Miller, J. Dunkel, A. C. Martin, *Dev. Cell* **2019**, *50*, 586.
- [187] A. Shellard, A. Szabo, X. Trepast, R. Mayor, *Science* **2018**, *362*, 339.
- [188] K. Roper, *Bioarchitecture* **2013**, *3*, 45.

- [189] E. Lang, C. Pedersen, A. Lang, P. Blicher, A. Klungland, A. Carlson, S. O. Boe, *Proc. Natl. Acad. Sci. U. S. A.* **2022**, *119*, e2201328119.
- [190] K. W. Rogers, A. F. Schier, *Annu. Rev. Cell Dev. Biol.* **2011**, *27*, 377.
- [191] H. Y. G. Lim, Y. D. Alvarez, M. Gasnier, Y. Wang, P. Tetlak, S. Bissiere, H. Wang, M. Biro, N. Plachta, *Nature* **2020**, *585*, 404.
- [192] Q. Chen, J. Shi, Y. Tao, M. Zernicka-Goetz, *Nat. Commun.* **2018**, *9*, 1819.
- [193] J. P. Winer, S. Oake, P. A. Janmey, *PLoS One* **2009**, *4*, e6382.
- [194] H. Safdari, A. Kalirad, C. Picioareanu, R. Tusserkani, B. Goliaei, M. Sadeghi, *PLoS One* **2020**, *15*, e0232060.
- [195] S. Huang, *Development* **2009**, *136*, 3853.
- [196] A. Schauer, D. Pinheiro, R. Hauschild, C. P. Heisenberg, *Elife* **2020**, *9*, 55190.
- [197] D. A. Turner, P. Baillie-Johnson, A. M. Arias, *BioEssays* **2016**, *38*, 181.
- [198] G. Martinez-Ara, N. Taberner, M. Takayama, E. Sandaltzopoulou, C. E. Villava, M. Bosch-Padros, N. Takata, X. Trepas, M. Eiraku, M. Ebisuya, *Nat. Commun.* **2022**, *13*, 5400.
- [199] M. Linde-Medina, R. Marcucio, *Prog. Biophys. Mol. Biol.* **2018**, *137*, 46.
- [200] C.-P. P. Heisenberg, Y. Bellaïche, *Cell* **2013**, *153*, 948.
- [201] E. Heller, E. Fuchs, *J. Cell Biol.* **2015**, *211*, 219.
- [202] A. E. Shyer, A. R. Rodrigues, G. G. Schroeder, E. Kassianidou, S. Kumar, R. M. Harland, *Science* **2017**, *357*, 811.
- [203] K. H. Palmquist, S. F. Tiemann, F. L. Ezzeddine, S. Yang, C. R. Pfeifer, A. Erzberger, A. R. Rodrigues, A. E. Shyer, *Cell* **2022**, *185*, 1960.
- [204] R. Cohen, L. Amir-Zilberstein, M. Hersch, S. Woland, O. Loza, S. Taiber, F. Matsuzaki, S. Bergmann, K. B. Avraham, D. Sprinzak, *Nat. Commun.* **2020**, *11*, 5137.
- [205] C. Bonnans, J. Chou, Z. Werb, *Nat. Rev. Mol. Cell Biol.* **2014**, *15*, 786.
- [206] M. Poujade, E. Grasland-Mongrain, A. Hertzog, J. Jouanneau, P. Chavrier, B. Ladoux, A. Buguin, P. Silberzan, *Proc. Natl. Acad. Sci. U. S. A.* **2007**, *104*, 15988.
- [207] X. Trepas, M. R. Wasserman, T. E. Angelini, E. Millet, D. A. Weitz, J. P. Butler, J. J. Fredberg, *Nat. Phys.* **2009**, *5*, 426.
- [208] D. T. Tambe, U. Crouelle, X. Trepas, C. Y. Park, J. H. Kim, E. Millet, J. P. Butler, J. J. Fredberg, *PLoS One* **2013**, *8*, e55172.
- [209] M. R. Ng, A. Besser, G. Danuser, J. S. Brugge, *J. Cell Biol.* **2012**, *199*, 545.
- [210] H. E. Balcioglu, L. Balasubramaniam, T. V. Stirbat, B. L. Doss, M. A. Fardin, R. M. Mege, B. Ladoux, *Soft Matter* **2020**, *16*, 1825.
- [211] C. G. Tusan, Y. H. Man, H. Zarkoob, D. A. Johnston, O. G. Andriotis, P. J. Thurner, S. Yang, E. A. Sander, E. Gentleman, B. G. Sengers, N. D. Evans, *Biophys. J.* **2018**, *114*, 2743.
- [212] A. Shellard, R. Mayor, *Nature* **2021**, *600*, 690.
- [213] A. G. Clark, A. Maitra, C. Jacques, M. Bergert, C. Perez-Gonzalez, A. Simon, L. Lederer, A. Diz-Munoz, X. Trepas, R. Voituriez, D. M. Vignjevic, *Nat. Mater.* **2022**, *21*, 1200.
- [214] A. Palamidessi, C. Malinverno, E. Frittoli, S. Corallino, E. Barbieri, S. Sigismund, G. V. Beznoussenko, E. Martini, M. Garre, I. Ferrara, C. Tripodo, F. Ascione, E. A. Cavalcanti-Adam, Q. Li, P. P. Di Fiore, D. Parazzoli, F. Giavazzi, R. Cerbino, G. Scita, *Nat. Mater.* **2019**, *18*, 1252.
- [215] C. L. Marchant, A. N. Malmi-Kakkada, J. A. Espina, E. H. Barriga, *Nat. Mater.* **2022**, *21*, 1314.
- [216] O. Ilina, P. G. Gritsenko, S. Syga, J. Lippoldt, C. A. M. La Porta, O. Chepizhko, S. Grosser, M. Vullings, G. J. Bakker, J. Starruss, P. Bult, S. Zapperi, J. A. Kas, A. Deutsch, P. Friedl, *Nat. Cell Biol.* **2020**, *22*, 1103.
- [217] M. J. Paszek, N. Zahir, K. R. Johnson, J. N. Lakins, G. I. Rozenberg, A. Gefen, C. A. Reinhart-King, S. S. Margulies, M. Dembo, D. Boettiger, D. A. Hammer, V. M. Weaver, *Cancer Cell* **2005**, *8*, 241.
- [218] O. Chaudhuri, S. T. Koshy, C. Branco da Cunha, J. W. Shin, C. S. Verbeke, K. H. Allison, D. J. Mooney, *Nat. Mater.* **2014**, *13*, 970.
- [219] T. Fuhs, F. Wetzel, A. W. Fritsch, X. Li, R. Stange, S. Pawlizak, T. R. Kießling, E. Morawetz, S. Grosser, F. Sauer, J. Lippoldt, F. Renner, S. Friebe, M. Zink, K. Bendrat, J. Braun, M. H. Oktay, J. Condeelis, S. Briest, B. Wolf, L.-C. Horn, M. Höckel, B. Aktas, M. C. Marchetti, M. L. Manning, A. Niendorf, D. Bi, J. A. Käs, *Nat. Phys.* **2022**, *18*, 1510.
- [220] Y. Jiang, H. Zhang, J. Wang, Y. Liu, T. Luo, H. Hua, *J. Hematol. Oncol.* **2022**, *15*, 34.
- [221] S. C. Wei, L. Fattet, J. H. Tsai, Y. Guo, V. H. Pai, H. E. Majeski, A. C. Chen, R. L. Sah, S. S. Taylor, A. J. Engler, J. Yang, *Nat. Cell Biol.* **2015**, *17*, 678.
- [222] L. Tweedy, P. A. Thomason, P. I. Paschke, K. Martin, L. M. Machesky, M. Zagnoni, R. H. Insall, *Science* **2020**, *369*, 9792.
- [223] L. Tweedy, R. H. Insall, *Front. Cell Dev. Biol.* **2020**, *8*, 133.
- [224] M. E. Todhunter, N. Y. Jee, A. J. Hughes, M. C. Coyle, A. Cerchiaro, J. Farlow, J. C. Garbe, M. A. LaBarge, T. A. Desai, Z. J. Gartner, *Nat. Methods* **2015**, *12*, 975.
- [225] E. D'Arcangelo, A. P. McGuigan, *BioTechniques* **2015**, *58*, 13.
- [226] S. Raghavan, R. A. Desai, Y. Kwon, M. Mrksich, C. S. Chen, *Langmuir* **2010**, *26*, 17733.
- [227] M. Vishwakarma, J. Di Russo, D. Probst, U. S. Schwarz, T. Das, J. P. Spatz, *Nat. Commun.* **2018**, *9*, 3469.
- [228] K. Vazquez, A. Saraswathibhatla, J. Notbohm, *Sci. Rep.* **2022**, *12*, 2474.
- [229] E. Anon, X. Serra-Picamal, P. Hersen, N. C. Gauthier, M. P. Sheetz, X. Trepas, B. Ladoux, *Proc. Natl. Acad. Sci. U. S. A.* **2012**, *109*, 10891.
- [230] S. R. Vedula, M. C. Leong, T. L. Lai, P. Hersen, A. J. Kabla, C. T. Lim, B. Ladoux, *Proc. Natl. Acad. Sci. U. S. A.* **2012**, *109*, 12974.
- [231] A. K. Marel, M. Zorn, C. Klingner, R. Wedlich-Soldner, E. Frey, J. O. Radler, *Biophys. J.* **2014**, *107*, 1054.
- [232] G. Peyret, R. Mueller, J. d'Alessandro, S. Begnaud, P. Marcq, R. M. Mege, J. M. Yeomans, A. Doostmohammadi, B. Ladoux, *Biophys. J.* **2019**, *117*, 464.
- [233] F. J. Segerer, F. Thüroff, A. Piera Alberola, E. Frey, J. O. Rädler, *Phys. Rev. Lett.* **2015**, *114*, 228102.
- [234] P. Costa, L. M. Blowes, A. C. Laly, J. T. Connelly, *Acta Biomater.* **2021**, *126*, 291.
- [235] S. Rausch, T. Das, J. R. D. Soiné, T. W. Hofmann, C. H. J. Boehm, U. S. Schwarz, H. Boehm, J. P. Spatz, *Biointerphases* **2013**, *8*, 32.
- [236] E. W. Gomez, Q. K. Chen, N. Gjorevski, C. M. Nelson, *J. Cell. Biochem.* **2010**, *110*, 44.
- [237] I. Jain, I. C. Berg, A. Acharya, M. Blaauw, N. Gosstola, P. Perez-Pinera, G. H. Underhill, *Commun Biol* **2022**, *5*, 1073.
- [238] K. B. Kaylan, I. C. Berg, M. J. Biehl, A. Brougham-Cook, I. Jain, S. M. Jamil, L. H. Sargeant, N. J. Cornell, L. T. Raetzman, G. H. Underhill, *Elife* **2018**, *7*.
- [239] J. M. Muncie, N. M. E. Ayad, J. N. Lakins, X. Xue, J. Fu, V. M. Weaver, *Dev. Cell* **2020**, *55*, 679.
- [240] T. B. Saw, A. Doostmohammadi, V. Nier, L. Kocgozlu, S. Thampi, Y. Toyama, P. Marcq, C. T. Lim, J. M. Yeomans, B. Ladoux, *Nature* **2017**, *544*, 212.
- [241] M. Deforet, V. Hakim, H. G. Yevick, G. Duclos, P. Silberzan, *Nat. Commun.* **2014**, *5*, 3747.
- [242] E. Latorre, S. Kale, L. Casares, M. Gomez-Gonzalez, M. Uroz, L. Valon, R. V. Nair, E. Garreta, N. Montserrat, A. Del Campo, B. Ladoux, M. Arroyo, X. Trepas, *Nature* **2018**, *563*, 203.
- [243] S. Blonski, J. Aureille, S. Badawi, D. Zaremba, L. Pernet, A. Grichine, S. Fraboulet, P. M. Korczyk, P. Recho, C. Guilly, M. E. Dolega, *Dev. Cell* **2021**, *56*, 3222.
- [244] M. Matejcic, X. Trepas, *Dev. Cell* **2020**, *54*, 569.
- [245] K. Shigetani, T. Fukuyama, R. Takahashi, K. Beppu, A. Tanaka, Y. T. Maeda, *RSC Adv.* **2022**, *12*, 20174.
- [246] B. Fabry, G. N. Maksym, J. P. Butler, M. Glogauer, D. Navajas, J. J. Fredberg, *Phys. Rev. Lett.* **2001**, *87*, 148102.

- [247] G. Lenormand, E. Millet, B. Fabry, J. P. Butler, J. J. Fredberg, *J. R. Soc. Interface* **2004**, *1*, 91.
- [248] N. Desprat, A. Richert, J. Simeon, A. Asnacios, *Biophys. J.* **2005**, *88*, 2224.
- [249] S. Weng, Y. Shao, W. Chen, J. Fu, *Nat. Mater.* **2016**, *15*, 961.
- [250] K. D. Webster, W. P. Ng, D. A. Fletcher, *Biophys. J.* **2014**, *107*, 146.
- [251] A. R. Harris, L. Peter, J. Bellis, B. Baum, A. J. Kabla, G. T. Charras, *Proc. Natl. Acad. Sci. U. S. A.* **2012**, *109*, 16449.
- [252] J. Duque, A. Bonfanti, J. Fouchard, E. Ferber, A. Harris, A. J. Kabla, G. T. Charras, *bioRxiv*, **2023**.
- [253] D. Stopak, A. K. Harris, *Dev Biol* **1982**, *90*, 383.
- [254] C. M. Nelson, M. M. VanDuijn, J. L. Inman, D. A. Fletcher, M. J. Bissell, *Science* **2006**, *314*, 298.
- [255] O. Iliina, G. J. Bakker, A. Vasaturo, R. M. Hofmann, P. Friedl, *Phys. Biol.* **2011**, *8*, 015010.
- [256] M. Nikolaev, O. Mitrofanova, N. Broguiere, S. Geraldo, D. Dutta, Y. Tabata, B. Elci, N. Brandenberg, I. Kolotuev, N. Gjorevski, H. Clevers, M. P. Lutolf, *Nature* **2020**, *585*, 574.
- [257] N. Gjorevski, C. M. Nelson, *Biophys. J.* **2012**, *103*, 152.
- [258] N. Gjorevski, A. S. Piotrowski, V. D. Varner, C. M. Nelson, *Sci. Rep.* **2015**, *5*, 11458.
- [259] C. M. Bidan, P. Kollmannsberger, V. Gering, S. Ehrig, P. Joly, A. Petersen, V. Vogel, P. Fratzl, J. W. Dunlop, *J. R. Soc. Interface* **2016**, *13*, 20160136.
- [260] P. Kollmannsberger, C. M. Bidan, J. W. C. Dunlop, P. Fratzl, V. Vogel, *Sci. Adv.* **2018**, *4*, 4881.
- [261] W. Xi, S. Sonam, T. Beng Saw, B. Ladoux, C. Teck Lim, *Nat. Commun.* **2017**, *8*, 1.
- [262] M. B. Mazalan, M. A. B. Ramlan, J. H. Shin, T. Ohashi, *Micromachines* **2020**, *11*, 659.
- [263] M. Zeng, S. Jin, K. Ye, *SLAS Technol.* **2018**, *23*, 301.
- [264] S. Panda, S. Hajra, K. Mistewicz, B. Nowacki, P. In-Na, A. Krushynska, Y. K. Mishra, H. J. Kim, *Biomater. Sci.* **2022**, *10*, 5054.
- [265] A. Trushko, I. Di Meglio, A. Merzouki, C. Blanch-Mercader, S. Abuhattum, J. Guck, K. Alessandri, P. Nassoy, K. Kruse, B. Chopard, A. Roux, *Dev. Cell* **2020**, *54*, 655.
- [266] K. Alessandri, M. Feyeux, B. Gurchenkov, C. Delgado, A. Trushko, K. H. Krause, D. Vignjevic, P. Nassoy, A. Roux, *Lab Chip* **2016**, *16*, 1593.
- [267] E. D. Lemma, B. Spagnolo, M. De Vittorio, F. Pisanello, *Trends Biotechnol.* **2019**, *37*, 358.
- [268] C. Fendler, C. Denker, J. Harberts, P. Bayat, R. Zierold, G. Loers, M. Munzenberg, R. H. Blick, *Adv. Biosyst.* **2019**, *3*, 1800329.
- [269] L. Agrawal, M. Saidani, L. Guillaud, M. Terenzio, *Mater. Sci. Eng., C* **2021**, *131*, 112502.
- [270] A. Sharaf, B. Roos, R. Timmerman, G. J. Kremers, J. J. Bajramovic, A. Accardo, *Front. Bioeng. Biotechnol.* **2022**, *10*, 926642.
- [271] N. Barin, H. E. Balcioglu, I. de Heer, M. de Wit, M. L. M. Lamfers, M. E. van Royen, P. J. French, A. Accardo, *Small* **2022**, *18*, 2204485.
- [272] A. M. Greiner, M. Jackel, A. C. Scheiwe, D. R. Stamow, T. J. Autenrieth, J. Lahann, C. M. Franz, M. Bastmeyer, *Biomaterials* **2014**, *35*, 611.
- [273] V. Hahn, P. Rietz, F. Hermann, P. Müller, C. Barner-Kowollik, T. Schlöder, W. Wenzel, E. Blasco, M. Wegener, *Nat. Photonics* **2022**, *16*, 784.
- [274] V. Hahn, T. Messer, N. M. Bojanowski, E. R. Curticean, I. Wacker, R. R. Schröder, E. Blasco, M. Wegener, *Nat. Photonics* **2021**, *15*, 932.
- [275] B. Ladoux, R. M. Mège, *Nat. Rev. Mol. Cell Biol.* **2017**, *18*, 743.
- [276] R. A. Foty, M. S. Steinberg, *Int. J. Dev. Biol.* **2004**, *48*, 397.
- [277] F. Graner, J. A. Glazier, *Phys. Rev. E* **1993**, *47*, 2128.
- [278] P. J. Albert, U. S. Schwarz, *PLoS Comput. Biol.* **2016**, *12*, e1004863.
- [279] F. Thüroff, A. Goychuk, M. Reiter, E. Frey, *Elife* **2019**, *8*, e46842.
- [280] A. Shirinifard, J. S. Gens, B. L. Zaitlen, N. J. Poplawski, M. Swat, J. A. Glazier, *PLoS One* **2009**, *4*, e7190.
- [281] R. Farhadifar, J. C. Röper, B. Aigouy, S. Eaton, F. Jülicher, *Curr. Biol.* **2007**, *17*, 2095.
- [282] J. Löber, F. Ziebert, I. S. Aranson, *Sci. Rep.* **2015**, *5*, 9172.
- [283] S. Alt, P. Ganguly, G. Salbreux, *Philos. Trans. R. Soc., B* **2017**, *372*, 20150520.
- [284] M. Osterfield, X. X. Du, T. Schüpbach, E. Wieschaus, S. Y. Shvartsman, *Dev. Cell* **2013**, *24*, 400.
- [285] M. Czajkowski, D. Bi, M. L. Manning, M. C. Marchetti, *Soft Matter* **2018**, *14*, 5628.
- [286] M. Nonomura, *PLoS One* **2012**, *7*, e33501.
- [287] R. Chojowski, U. S. Schwarz, F. Ziebert, *Eur. Phys. J. Spec. Top.* **2020**, *43*, 63.
- [288] J. Drost, H. Clevers, *Nat. Rev. Cancer* **2018**, *18*, 407.
- [289] H. Clevers, *Cell* **2013**, *154*, 274.
- [290] Y. Wang, D. B. Gunasekara, M. I. Reed, M. DiSalvo, S. J. Bultman, C. E. Sims, S. T. Magness, N. L. Allbritton, *Biomaterials* **2017**, *128*, 44.
- [291] D. Serra, U. Mayr, A. Boni, I. Lukonin, M. Rempfler, L. Challet Meylan, M. B. Stadler, P. Strnad, P. Papasaikas, D. Vischi, A. Waldt, G. Roma, P. Liberali, *Nature* **2019**, *569*, 66.
- [292] Q. Yang, S. L. Xue, C. J. Chan, M. Rempfler, D. Vischi, F. Maurer-Gutierrez, T. Hiiragi, E. Hannezo, P. Liberali, *Nat. Cell Biol.* **2021**, *23*, 733.
- [293] C. Perez-Gonzalez, G. Ceada, F. Greco, M. Matejic, M. Gomez-Gonzalez, N. Castro, A. Menendez, S. Kale, D. Krndija, A. G. Clark, V. R. Gannavarapu, A. Alvarez-Varela, P. Roca-Cusachs, E. Batlle, D. M. Vignjevic, M. Arroyo, X. Trepac, *Nat. Cell Biol.* **2021**, *23*, 745.
- [294] A. R. Abdel Fattah, B. Daza, G. Rustandi, M. A. Berrocal-Rubio, B. Gorissen, S. Poovathingal, K. Davie, J. Barrasa-Fano, M. Condor, X. Cao, D. H. Rosenzweig, Y. Lei, R. Finnell, C. Verfaillie, M. Sampaolesi, P. Dedecker, H. van Oosterwyck, S. Aerts, A. Ranga, *Nat. Commun.* **2021**, *12*, 3192.
- [295] G. T. Knight, B. F. Lundin, N. Iyer, L. M. Ashton, W. A. Sethares, R. M. Willett, R. S. Ashton, *Elife* **2018**, *7*, e37549.
- [296] K. Taniguchi, Y. Shao, R. F. Townshend, Y. H. Tsai, C. J. DeLong, S. A. Lopez, S. Gayen, A. M. Freddo, D. J. Chue, D. J. Thomas, J. R. Spence, B. Margolis, S. Kalantry, J. Fu, K. S. O'Shea, D. L. Gumucio, *Stem Cell Rep.* **2015**, *5*, 954.
- [297] Q. Li, Y. Zhang, P. Pluchon, J. Robens, K. Herr, M. Mercade, J. P. Thiery, H. Yu, V. Viasnoff, *Nat. Cell Biol.* **2016**, *18*, 311.
- [298] T. Haremaki, J. J. Metzger, T. Rito, M. Z. Ozair, F. Etoc, A. H. Brivanlou, *Nat. Biotechnol.* **2019**, *37*, 1198.
- [299] M. A. Lancaster, N. S. Corsini, S. Wolfinger, E. H. Gustafson, A. W. Phillips, T. R. Burkard, T. Otani, F. J. Livesey, J. A. Knoblich, *Nat. Biotechnol.* **2017**, *35*, 659.
- [300] S. H. Kim, S. K. Im, S. J. Oh, S. Jeong, E. S. Yoon, C. J. Lee, N. Choi, E. M. Hur, *Nat. Commun.* **2017**, *8*, 1.
- [301] A. Petersen, A. Princ, G. Korus, A. Ellinghaus, H. Leemhuis, A. Herrera, A. Klaumunzer, S. Schreivogel, A. Woloszyk, K. Schmidt-Bleek, S. Geissler, I. Heschel, G. N. Duda, *Nat. Commun.* **2018**, *9*, 4430.
- [302] W. Han, R. el Botty, E. Montaudon, L. Malaquin, F. Deschaseaux, N. Espagnolle, E. Marangoni, P. Cottu, G. Zalcmann, M. C. Parrini, F. Assayag, L. Sensebe, P. Silberzan, A. Vincent-Salomon, G. Dutertre, S. Roman-Roman, S. Descroix, J. Camonis, *Biomaterials* **2021**, *269*, 120624.
- [303] A. Raic, L. Rodling, H. Kalbacher, C. Lee-Thedieck, *Biomaterials* **2014**, *35*, 929.
- [304] V. Bondarenko, M. Nikolaev, D. Kromm, R. Belousov, A. Wolny, S. Rezakhani, J. Hugger, V. Uhlmann, L. Hufnagel, A. Kreshuk, J. Ellenberg, A. Erzberger, M. Lutolf, T. Hiiragi, *bioRxiv*, **2022**.
- [305] K. O. Okeyo, M. Tanabe, O. Kurosawa, H. Oana, M. Washizu, *Dev. Growth Differ.* **2018**, *60*, 183.
- [306] S. Randriamanantsoa, A. Papargyriou, H. C. Maurer, K. Peschke, M. Schuster, G. Zecchin, K. Steiger, R. Ollinger, D. Saur, C. Scheel, R.

- Rad, E. Hannezo, M. Reichert, A. R. Bausch, *Nat. Commun.* **2022**, *13*, 5219.
- [307] N. Broguiere, L. Isenmann, C. Hirt, T. Ringel, S. Placzek, E. Cavalli, F. Ringnald, L. Villiger, R. Zullig, R. Lehmann, G. Rogler, M. H. Heim, J. Schuler, M. Zenobi-Wong, G. Schwank, *Adv. Mater.* **2018**, *30*, 1801621.
- [308] B. Kong, Y. Chen, R. Liu, X. Liu, C. Liu, Z. Shao, L. Xiong, X. Liu, W. Sun, S. Mi, *Nat. Commun.* **2020**, *11*, 1435.
- [309] Z. Ma, J. Wang, P. Loskill, N. Huebsch, S. Koo, F. L. Svedlund, N. C. Marks, E. W. Hua, C. P. Grigoropoulos, B. R. Conklin, K. E. Healy, *Nat. Commun.* **2015**, *6*, 7413.
- [310] A. Phuong Le, J. Kim, K. R. Koehler, *Development* **2022**, *149*, 7.
- [311] M. Campisi, Y. Shin, T. Osaki, C. Hajal, V. Chiono, R. D. Kamm, *Bio-materials* **2018**, *180*, 117.
- [312] M. A. Skylar-Scott, S. G. M. Uzel, L. L. Nam, J. H. Ahrens, R. L. Truby, S. Damaraju, J. A. Lewis, *Sci. Adv.* **2019**, *5*, eaaw2459.
- [313] K. A. Homan, N. Gupta, K. T. Kroll, D. B. Kolesky, M. Skylar-Scott, T. Miyoshi, D. Mau, M. T. Valerius, T. Ferrante, J. V Bonventre, J. A. Lewis, R. Morizane, *Nat. Methods* **2019**, *16*, 255.
- [314] T. Ching, J. Vasudevan, S. Y. Chang, H. Y. Tan, A. Sargur Ranganath, C. T. Lim, J. G. Fernandez, J. J. Ng, Y. C. Toh, M. Hashimoto, *Small* **2022**, *18*, 2203426.
- [315] S. Montes-Olivas, L. Marucci, M. Homer, *Front. Genet.* **2019**, *10*, 873.
- [316] S. Okuda, Y. Inoue, T. Watanabe, T. Adachi, *Interface Focus* **2015**, *5*, 20140095.
- [317] S. Okuda, N. Takata, Y. Hasegawa, M. Kawada, Y. Inoue, T. Adachi, Y. Sasai, M. Eiraku, *Sci. Adv.* **2018**, *4*, 2386.
- [318] S. Okuda, T. Miura, Y. Inoue, T. Adachi, M. Eiraku, *Sci. Rep.* **2018**, *8*, 2386.
- [319] B. Cerruti, A. Puliafito, A. M. Shewan, W. Yu, A. N. Combes, M. H. Little, F. Chianale, L. Primo, G. Serini, K. E. Mostov, A. Celani, A. Gamba, *J. Cell Biol.* **2013**, *203*, 359.
- [320] C. Pin, A. Parker, A. P. Gunning, Y. Ohta, I. T. Johnson, S. R. Carding, T. Sato, *Integr. Biol.* **2015**, *7*, 213.
- [321] H. Yan, A. Konstorum, J. S. Lowengrub, *Bull. Math. Biol.* **2018**, *80*, 1404.
- [322] P. Buske, J. Przybilla, M. Loeffler, N. Sachs, T. Sato, H. Clevers, J. Galle, *FEBS J.* **2012**, *279*, 3475.
- [323] T. Thalheim, M. Quaas, M. Herberg, U. D. Braumann, C. Kerner, M. Loeffler, G. Aust, J. Galle, *Dev. Biol.* **2018**, *433*, 254.
- [324] E. Berger, C. Magliaro, N. Paczia, A. S. Monzel, P. Antony, C. L. Linster, S. Bolognin, A. Ahluwalia, J. C. Schwamborn, *Lab Chip* **2018**, *18*, 3172.



Rabea Link is currently a Ph.D. student at Heidelberg University at the Institute of Theoretical Physics and at the BioQuant-Center for Quantitative Biology. She received her B.Sc. and M.Sc. degrees in physics in 2017 and 2019, respectively, at Heidelberg University. In her research, she uses 3D models, such as the cellular Potts model, to describe the shape and dynamics of single cells and cell collectives in geometrically structured environments.



Kai Weißenbruch until early 2023 was a postdoctoral researcher at the Zoological Institute, Department of Cell- and Neurobiology, of the Karlsruhe Institute of Technology (KIT), where he also received his B.Sc., M.Sc., and Ph.D. degrees. He currently works as a postdoctoral researcher with Roberto Mayor at University College London (UCL). His research focuses on cellular mechanobiology. In particular, he uses state-of-the-art microfabrication techniques and cutting-edge microscopy to control cell shape and monitor cellular force generation in single cells.



Motomu Tanaka is a professor of biophysical chemistry at Heidelberg with a special focus on the mechanics and dynamics of soft and biological interfaces. He received his Ph.D. from Kyoto University in physical chemistry in 1998 and moved to Technical University Munich as a postdoc under the mentorship of Erich Sackmann. He led an Emmy Noether independent research group and received his habilitation degree in experimental physics. He moved to Heidelberg in 2005. Since 2013, in addition, he also leads a research group at Kyoto University in Japan.



Martin Bastmeyer is a professor of cell and neurobiology at the Karlsruhe Institute of Technology (KIT). He received his Ph.D. in 1989 for work at the Max Planck Institute for Biology in Tübingen and then worked as a postdoc at the Salk Institute in San Diego, USA. Later he received his habilitation degree and was an independent Heisenberg fellow at the University of Konstanz. From 2001 to 2004 he was a professor of neurobiology at the University of Jena. He moved to Karlsruhe in 2004, where he is also one of the directors of the Institute for Biological and Chemical Systems. His research focuses on developmental biology, cell adhesion and mechanics, and advanced optical microscopy.



Ulrich Schwarz is a professor of theoretical physics at Heidelberg University, with a background in statistical, soft matter, and biological physics. He received his Ph.D. in 1998 for work at the Max Planck Institute of Colloids and Interface in Potsdam and then spent two years as a Minerva postdoctoral fellow at the Weizmann Institute in Israel. After leading an Emmy Noether junior research group on modeling cell adhesion at Potsdam and Heidelberg, in 2008 he was appointed professor for theoretical biophysics at the Karlsruhe Institute of Technology (KIT). He moved to Heidelberg in 2009.